PERGAMON

Deep-Sea Research II 46 (1999) 245–278

DEEP-SEA RESEARCH
PART II

Long-term hydrographic changes at 52 and 66°W in the North Atlantic Subtropical Gyre & Caribbean

Terrence M. Joyce*, Robert S. Pickart, Robert C. Millard

Woods Hole Oceanographic Institution, 360 Woods Hole Rd., Mail Stop 21, Woods Hole, MA 02543, USA

Received 5 December 1997; received in revised form 22 May 1998

Abstract

In July–September 1997 two hydrographic lines were done in the western N. Atlantic along longitudes of 52 and 66°W as part of the WOCE one-time hydrographic survey of the oceans. Each of these two lines approximately repeated earlier ones done during the International Geophysical Year(s) (IGY) and the mid-1980s. Because of this repeated sampling, long-term hydrographic changes in the water masses can be examined. In this report, we focus on temperature and salinity changes within the subtropical gyre mainly between latitudes of 20 and 35°N and compare our results to those presented by Bryden et al. (1996), who examined changes along a zonal line at 24°N, most recently occupied in 1992. Since this most recent 24°N section in 1992, substantial changes have occurred in the western part of the subtropical gyre at the depths of the Labrador Sea Water (LSW). In particular, we see clear evidence for colder, fresher Labrador Sea Water throughout the gyre on our two recent sections that was not yet present in 1992 at similar longitudes along 24°N. At shallower depths inhabited by waters that are an admixture of Mediterranean (MW) and Antarctic Intermediate Waters (AAIW), our recent survey shows an increase in salinity, which can only be attributed to changes in water masses on potential temperature or neutral density surfaces. Furthermore, waters above the MW/AAIW layer and into the deeper part of the main pycnocline have continued to become saltier and warmer throughout the 40-year period spanned by our sections. These latter changes have been dominantly due to a vertical sinking of density surfaces as T/S changes in density surfaces are small, but depths of individual T/S horizons have increased with time. The net change since the IGY shows a mean temperature increase between 800 and 2500 m depth at a rate of 0.57°C/century with a corresponding steric sea level rise of 1 mm/yr, and a net downward heave with small values near the top and bottom, and a maximum rate of −2.7 m/yr at 1800 m depth. Changes in the deep Caribbean indicate a warming since the IGY due to

*Corresponding author. Tel.: 001 508 289 2530; fax: 001 508 457 2181; e-mail: tjoyce@whoi.edu.

PII: S0967-0645(98)00102-7

temperature increases of the inflowing source waters in the subtropical gyre at 1800m depth, but no significant change in the deep salinity.

1. Introduction

Two meridional hydrographic sections were made in the N. Atlantic at longitudes of 52 and 66°W from the N. American coast to S. America, with the latter section including the Caribbean. These sections, taken as part of the WOCE hydrographic program (WHP) one-time survey, included a number of tracer measurements (e.g. CFCs, radiocarbon, ^{3}He, nutrients) collected from a 36-bottle, 10-l rosette system and were, in part, chosen at the above longitudes because they repeated earlier long sections made during the IGY (1954–58) and in the 1980s (Table 1, Fig. 1). Our principal interest in this report is the changes that have occurred over time since the IGY, and therefore we will not report on the complete (including tracers) hydrographic data set here. In fact, we have limited ourselves to the vertical resolution of the hydrographic sampling (typically 30 levels in 5000 m depth so as to compare more appropriately with the IGY (1954–58) data, for which no continuous CTD data exist. Previous studies in the N. Atlantic using hydrographic sections (Roemmich and Wunsch, 1984; Bryden et al., 1996) have compared zonal sections. A different, but related, approach was used by Levitus (1989a, b) who analyzed intermediate and deep changes in the N. Atlantic from hydrographic station data taken in two different epochs. In the Bryden et al., study, three zonal sections at 24°N also spanned the IGY/80s/WOCE eras, but between the occupation of the most recent section in 1992 and the present, significant changes are to be expected in the western N. Atlantic based on recent cooling in the Labrador Sea (Lazier, 1995) and penetration of this signal into the subtropical gyre (Joyce and Robbins, 1996; Curry et al., 1998).

Table 1
Hydrographic Data from three eras used in our analysis of temporal changes

	Ship/Cruise/Leg	Dates	Longitude (nominal)
IGY CRUISES			
	Atlantis 208 Leg 1	(9/19/54–9/26/54)	~66W
	Atlantis 212 Leg 1	(11/11/54–12/13/54)	~66W
	Atlantis 229 Leg 1	(11/12/56–12/12/56)	~50W
	Crawford 17 Leg 1	(2/11/58–3/20/58)	~64W and ~66W
80s CRUISES			
	Oceanus 133 Leg 7	(5/1/83–5/17/83)	~52W
	Endeavor 129 Leg 1	(4/11/85–4/28/85)	~64W
WOCE CRUISES			
	Knorr 151 Leg 3	(7/1/97–8/9/97)	~52W
	Knorr 151 Leg 4	(8/16/87–9/3/97)	~66W

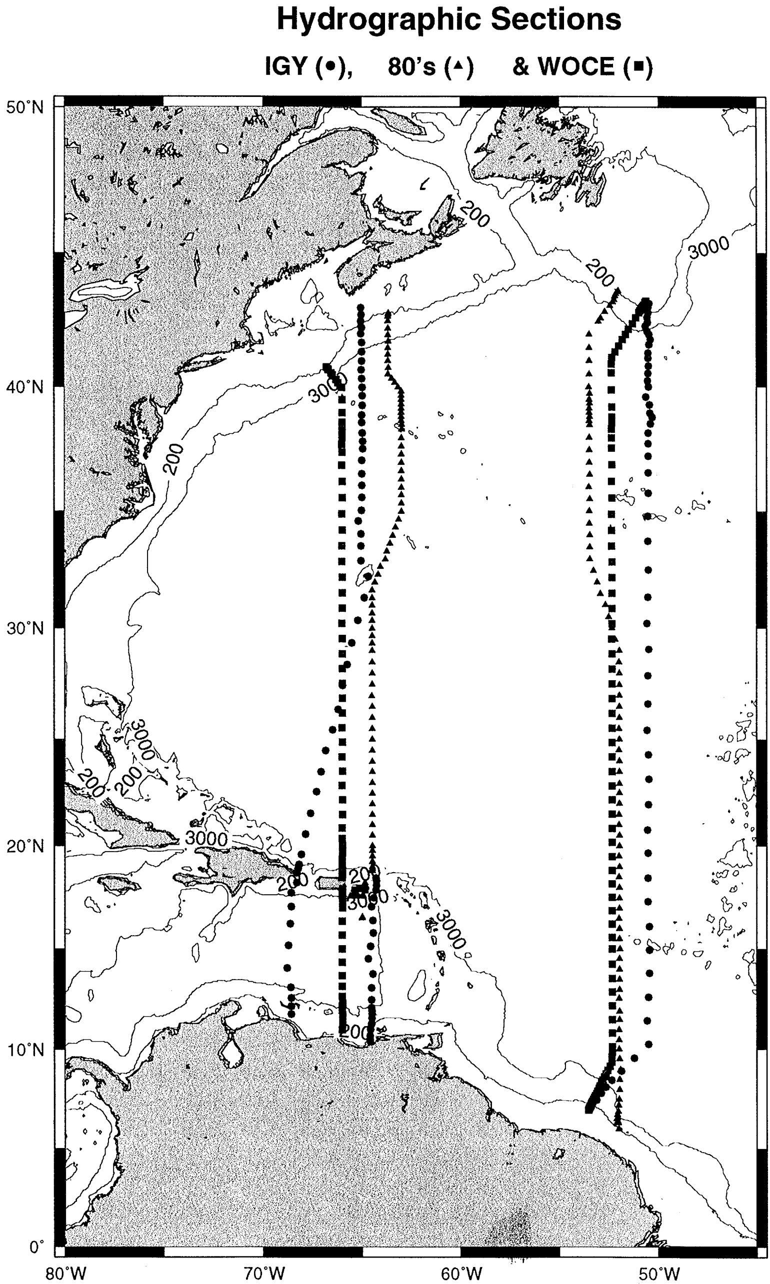

Fig. 1. Station plot of IGY, 80s and WOCE stations (see table 1 for cruises and dates). For reference, we show the 200 and 3000 m isobaths.

We begin this analysis by first presenting the overall temperature, salinity and density structure along the two meridians so that changes can be referenced to the basic hydrographic structure and water masses of the subtropical gyre. We follow this by showing differences between the sections in latitude depth space as well as averages over a range of latitudes. Next the mean changes are examined both in depth, T/S and neutral density space in order to quantify the nature of any significant change over time. Finally, changes in the Caribbean will be discussed in light of observed variability in the subtropical gyre.

2. Recent data from WOCE

The CTD system used on both legs consisted of a Mark IIIb 'Neil Brown' CTD with a dissolved oxygen sensor modified with an improved pressure sensor (Millard et al., 1993). A 36-place General Oceanics pylon with 36 'Scripps-type' water sampling bottles collected 10 l of water per sample. Stations were made to within several meters of the bottom except over the Puerto Rico Trench, where we limited our depth to 6000 m. Horizontal spacing between stations was nominally 30 nm, but was increased within the subtropical gyre and decreased near boundaries or in the Gulf Stream.

Calibration of the CTD indicated a traceable absolute calibration of temperature of 0.002°C, pressure of 2 dbar and salinity (using bottles samples run on a Guildline Autosal) of 0.001. All temperatures are reported in ITS90 units, although we note that in each of the three eras, a different temperature scale was used. The accuracy of the water sample salinities is tied directly to the accuracy of the Standard Seawater (SSW) batches which standardize the salinometer as well as the performance of the salinometer. The Atlantic Ocean Atlas (Fuglister, 1960) gives a salinity precision of $\pm$ 0.005 psu for IGY salinities but doesn't indicate the SSW batches used to analyze the salinities of these IGY sections, which will ultimately determine the accuracy of the salinity measurements. The IGY salinities along 66 W north of Bermuda were analyzed using titrations, not the present conductivity bridge; these titrated results have a precision of $\pm$ 0.02 psu. The bottle salts of the two modern CTD sections done in the early 1980s and again in 1997 along 52 and 66 W were analyzed on a Guildline Autosal Model 8400 salinometer in a temperature controlled area, see Knapp and Stalcup (1987). The sections in the early 1980s used standard water batch number P93 for both cruises, and the 1997 sections where done on consecutive legs of the Knorr cruise using a single SSW batch number P131. SSW batch P93 was compared with other SSW batches by Mantyla (1987) and found to require a slight salinity correction of $+$ 0.0004 psu. A post-cruise comparison of SSW batch P131 to P128 done at Woods Hole Oceanographic Institution shows, after correcting P128 for a time drift of $+$ 0.002 psu (Culkin and Ridout, 1998), that both SSW batch P131 and P93 have a negative difference of less than $-$ 0.0005 psu. The difference between batch P93 minus P131 is therefore found to be only $-$ 0.0001 psu, which is significantly less than the observed salinity differences, as we shall see later. Finally, the accuracy of modern SSW is estimated at better than $\pm$ 0.001 psu (Culkin and Ridout). A determination of accuracy of the IGY salinities is more an issue of systematic error than precision, as we will be dealing only with gross averages. Mantyla's (1980) documentation of early, post-titration, SSW variability leads us to expect possible systematic errors of ± 0.004 psu. Unfortunately, none of our sections ventured into the Canary Basin, where Saunders (1986) hypothesizes that no long-term changes in deep water properties occur and therefore systematic errors in measurement techniques can be examined. Finally, we have made no adjustments reflecting changes in the definition of salinity, as these are negligible in the oceanic range around 35 psu or 35 g/kg.

Since our goal is to compare hydrographic sections taken at different times, but not at exactly the same meridional locations, we need first to put all data onto a common grid. We have chosen depth and latitude, and have linearly interpolated the bottle data onto a uniform depth grid of 50 m resolution followed by projection onto a latitude grid of 0.5° resolution. The vertical interpolation of bottle data onto a higher resolution grid will introduce 'noise' into our gridded fields. Because the IGY bottle spacing resulted in only about 25 levels sampled, this interpolation problem is more severe. We have examined this source of error for both random and systematic effects: the former due to finestructure in the ocean and the latter due to curvature in the T/S profiles versus depth. Since we grid data from all three cruises based on 'bottle' or standard depths, the curvature bias is reduced in the differences, because all fields have a similar bias, which is of magnitude (0.1°C, 0.01 psu) or less in the upper 1500 m and much smaller in the deep water. The resulting errors in the section differences are largely random and of smaller magnitude than the typical 'eddy' noise. The horizontal gridding is consistant with the sampling over much of the domain; near boundaries or in the Gulf Stream, greater resolution is needed, and in fact available. However, our present study deals with broad-scale changes, which are readily seen with the above resolution. Prior to plotting, the data were smoothed using a 100-km wide gaussian filter. We note in advance of the temporal comparisons that we will ignore any small-scale zonal differences that might exist, as the sections are not all on a common longitude. Studies by Arbic and Owens (personal communication, 1997) indicate that away from major topographic features and strong currents, sampling errors due to this section offset are generally small compared with the eddy signal within each section.

We show the overall potential temperature, salinity and density structure observed on the two sections in Figs. 2 and 3. We have used the neutral density algorithm of Jackett and McDougall (1996) as the 'density' variable throughout this report. It closely approximates numerical values of potential density in the upper ocean and can be used throughout the water column.

The section at 52°W (WHP designation A20) shows the coldest waters of Antarctic Bottom Water (AABW) origin banked up to the south in the region between the continental slope and the mid-Atlantic Ridge. In this same region, the other major Antarctic water mass, Antarctic Intermediate Water (AAIW), most easily stands out as a salinity minimum layer at a depth of about 1000 m To the north of 20°N, the salinity at this depth increases as more influence of the salty Mediterranean Water (MW) outflow is found. To the north of the Gulf Stream (at approx. 38°N) a warm-core ring is present that has displaced the fresher Slope Water and Labrador Sea Water (LSW) to the north against the continental slope SW of the Grand Banks. We

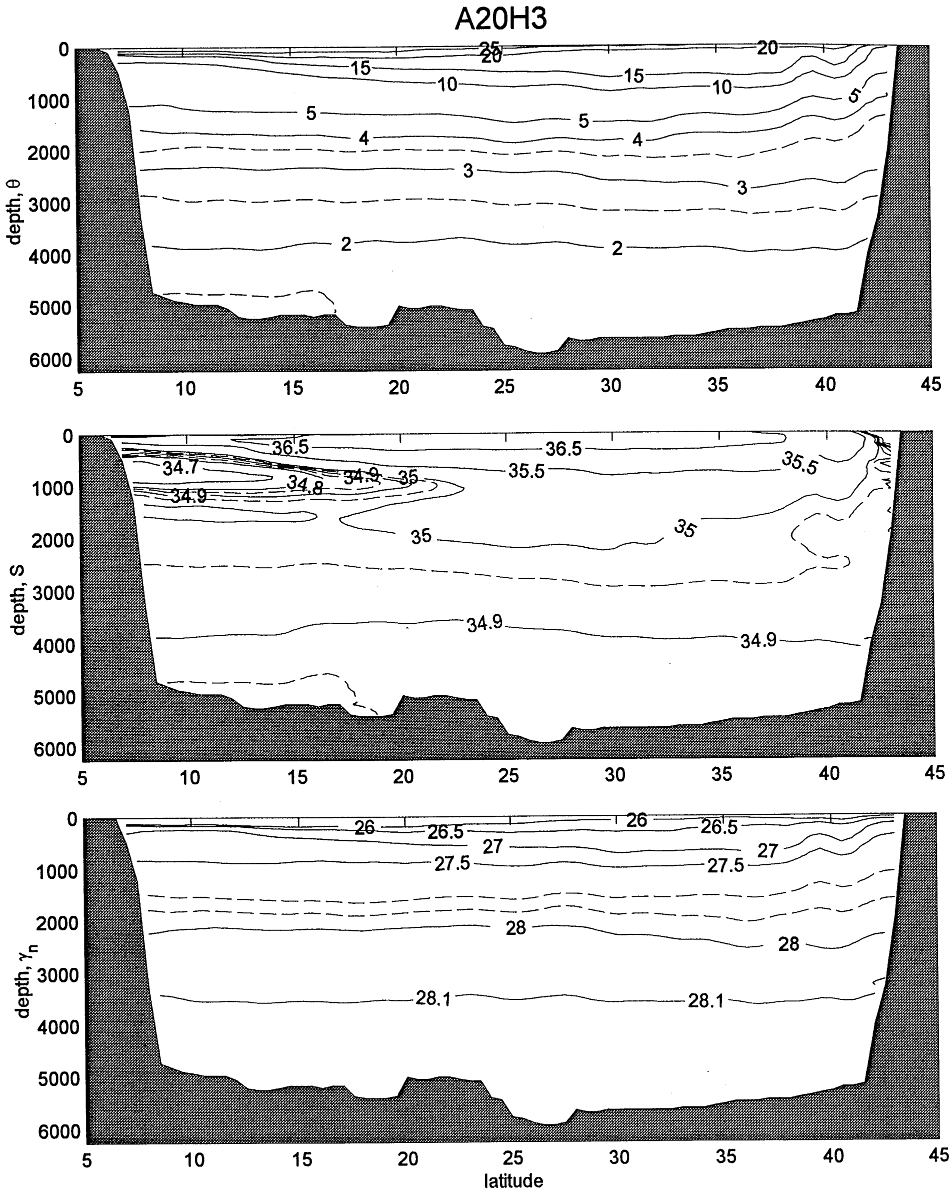

Fig. 2. The third and most recent (WOCE) section at 52 W (A20) for potential temperature (°C, upper panel), salinity and neutral density (kg/m^3, lower panel). Dashed contours for upper panel are for $\theta = 1.5$, 2.5 and 3.5°C, middle panel for $S = 34.85$, 34.95 and lower panel for $\gamma_n = 27.9$, 27.95 kg/m^3.

have indicated the core and upper density of the LSW by the dashed contours at 27.95 and 27.9 kg m^{-3}, respectively. On the core level density of LSW, the coldest and freshest water encountered on the section is over the continental slope to the north, with the warmest, saltiest water in the center of the section near 24°N. Further to the

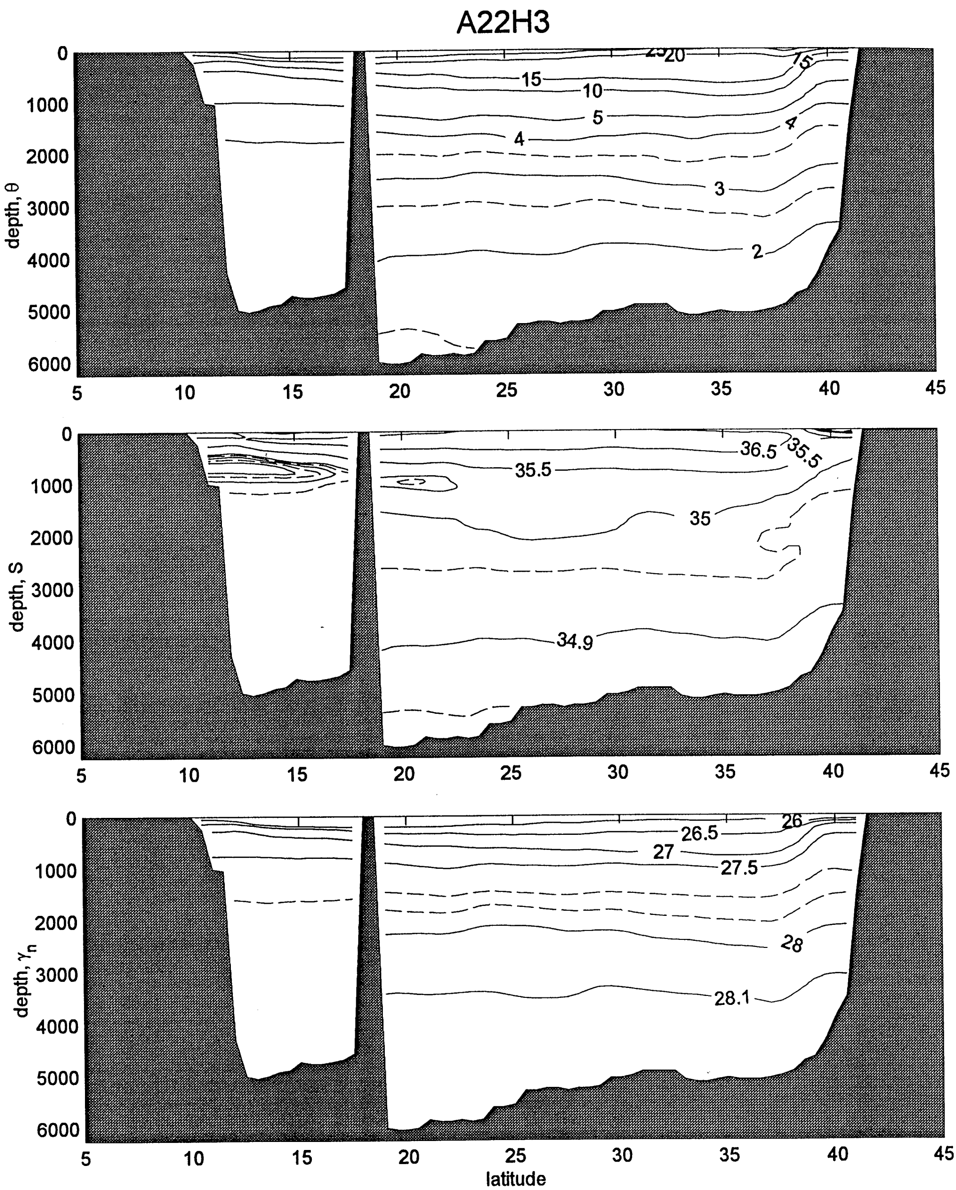

Fig. 3. Same as Fig. 2, but for 66 W (A22) section.

west along 66° W (WHP line A22, Fig. 3), the deep water of the Caribbean is seen to be vertically homogeneous below about 1800 m, the deepest sill depth for inflow of Atlantic water into the basin. This occurs through the Anegada-Junfern (AJ) Passage, just to the east of the section (Stalcup et al., 1975). Above this relatively homogeneous layer, the largest AAIW water signal is seen in the southern part of the basin, with an indication of lower salinity water to the north of Puerto Rico than is found immediately to the south, suggesting a second pathway for AAIW into the subtropical gyre besides the AJ Passage. On both sections, the influence of subtropical mode water (STMW, with a temperature of 18°C) can be seen by the thickening of the temperature contours between 15 and 20°C. This layer has a neutral density of approximately 26.5 $\mathrm{kg\,m^{-3}}$, nearly the same as the potential density of the layer first identified by Worthington (1959).

3. Changes observed over three eras for both sections

3.1. Depth/latitude changes

Our notation for changes in a variable C between occupations of a later section j compared to an earlier section i are denoted as δC_{ij} and are presented for potential temperature (θ) and salinity (S); these are shown for the two sections in Figs. 4 and 5. The previous studies comparing the IGY and 80 s data noted the apparent warming of the N. Atlantic at mid-depths (1000–2500 m), which is also evident in both the A20 and A22 sections (Figs. 4a and 5a, upper panels). However, comparing the 80s and WOCE data, this warming, especially at depths of 2000 m (near the core of the LSW) has largely ended (Figs. 4a and 5a, middle panels), although the net change from the IGY to the present still shows a basin-wide increase over this depth range. One must examine with care any changes near regions of strongly sloping isotherms such as the Gulf Stream, as differences in location of the front at the times of the sections will dominate the signal there. Thus, from a simple display of property change vs. depth one cannot say with any surety what, if any, change has occurred in these regions.

Like temperature differences, the salinity change from the IGY to the 80s at mid-depths, is positive and of broad scale. Recent changes since the 80s indicate that the LSW layer has become fresher, especially in the northern part of the section: in fact so much so that the net change from IGY to the present is negative at 2000 m to the north of 30°N in the A20 section and north of 35°N in A22. Again, changes near the boundaries and strong property gradients can be dominated by meandering and are not easily interpretable. Despite the salinity decrease since the 80s in the LSW layer near 2000 m, one can still see a broad scale net salinity increase in both sections above this layer between depths of 1000 and 1500 m. In the deepest water, one generally sees a salinity decrease with time from the IGY to the present.

3.2. Mean property changes between 20 and 35°N

In order to document the large-scale changes within the basin, we have chosen to average the data between latitude bounds of 20 and 35°N. On the A20 section, this window eliminates the strong latitudinal gradients in the AAIW water and masks out the coldest AABW layer as well. It will be more convenient to consider this deepest layer Lower Deep Water (LDW) following McCartney (1992), recognizing that it is

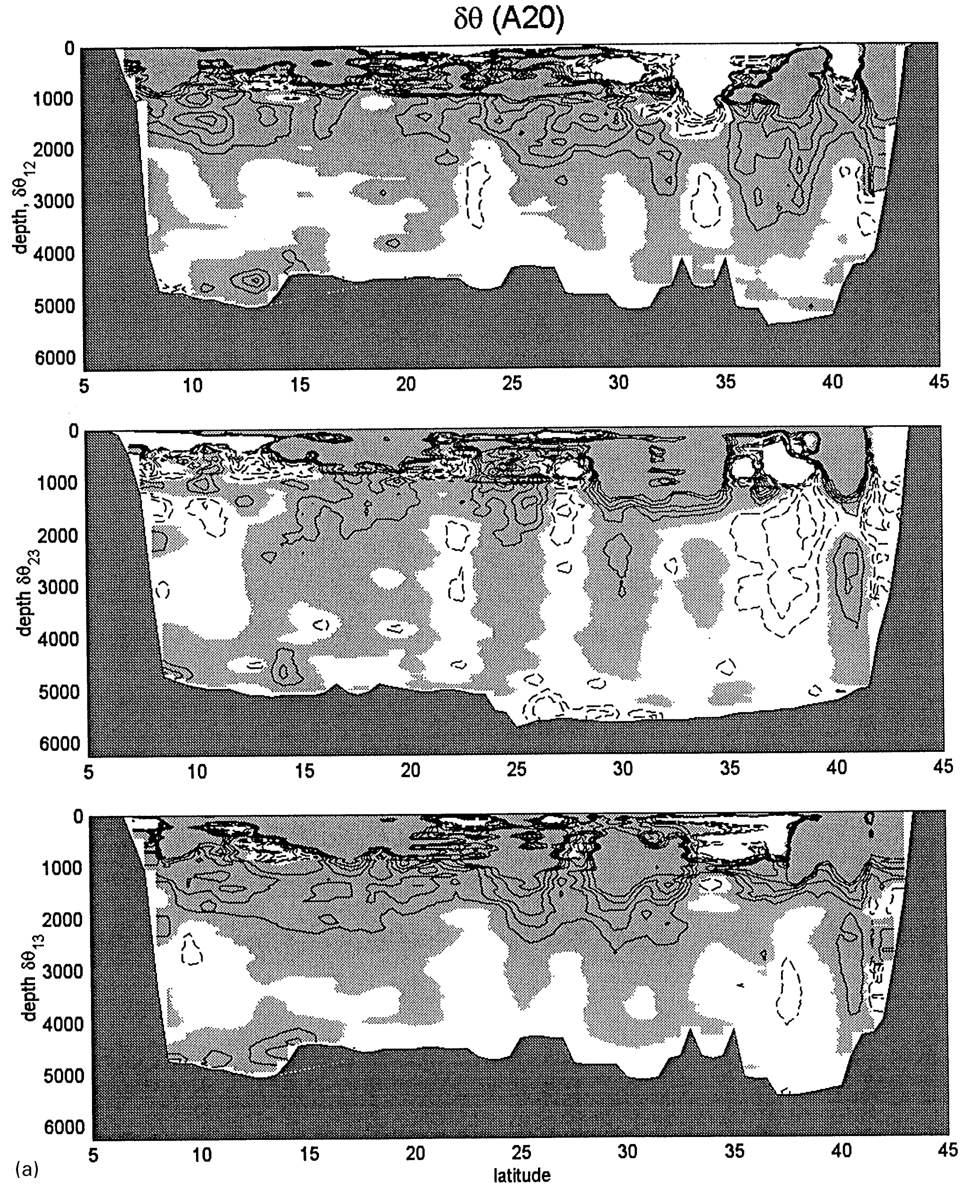

Fig. 4. A20 potential temperature differences for 80s-IGY (upper), WOCE-80s (middle) and WOCE-IGY (lower). Positive differences are in gray with the contour interval of 0.1 up to a maximum (minimum) of 0.5 (− 0.5) (a). As above but for salinity differences with the contour interval of 0.02 up to a maximum (minimum) of 0.1 (− 0.1) (b).

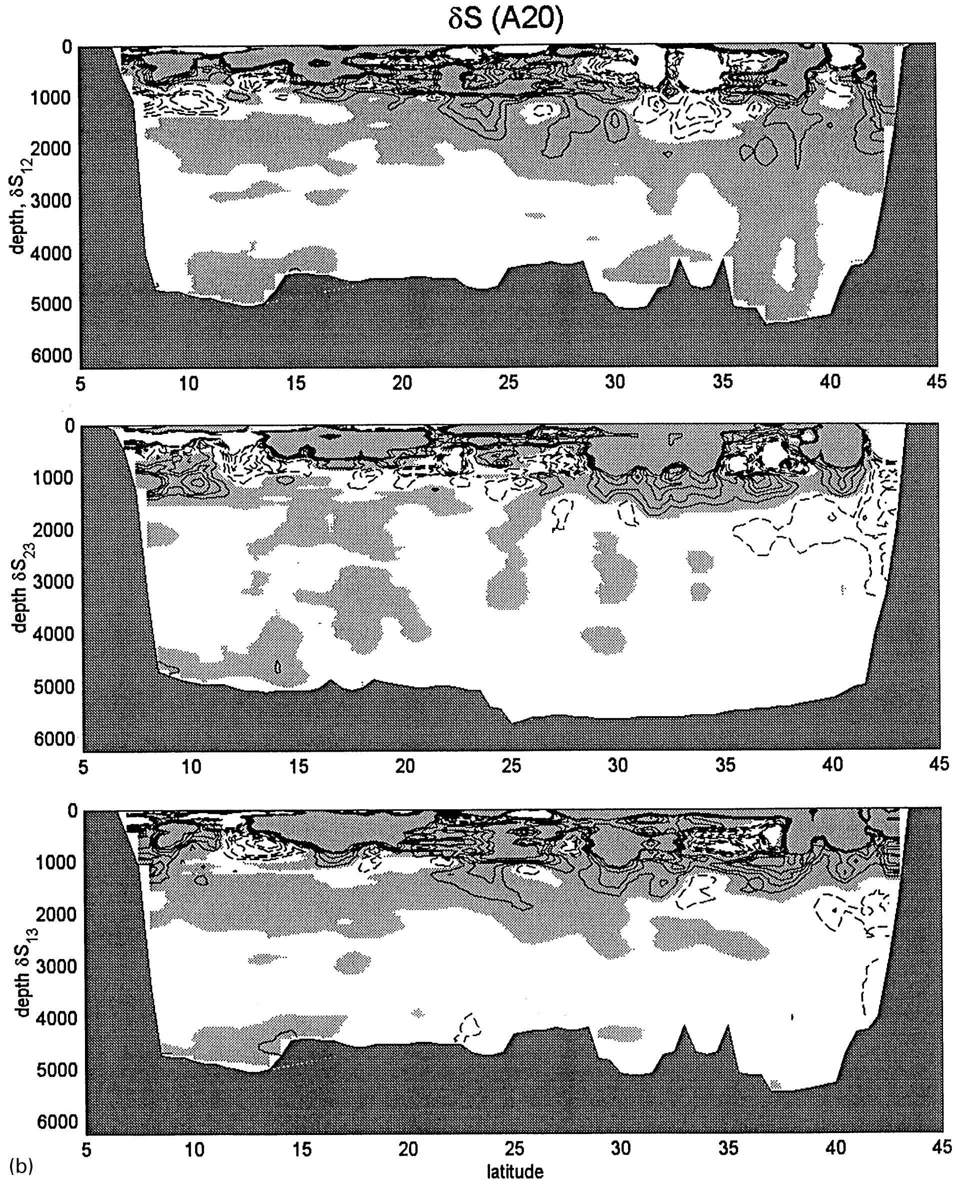

Fig. 4. Continued.

a varying mix of overflow waters from the Nordic Seas and AABW. On A22, changes in the coldest version of the LDW are within the latitude window of 20 and 35°N, while on A20 they are not. Mean differences for each section are presented in Figs. 6 and 7, with an error in the mean estimate based on a 300 km eddy scale and five degrees of freedom as in Parrilla et al. (1994). While this scale is larger than a radius of

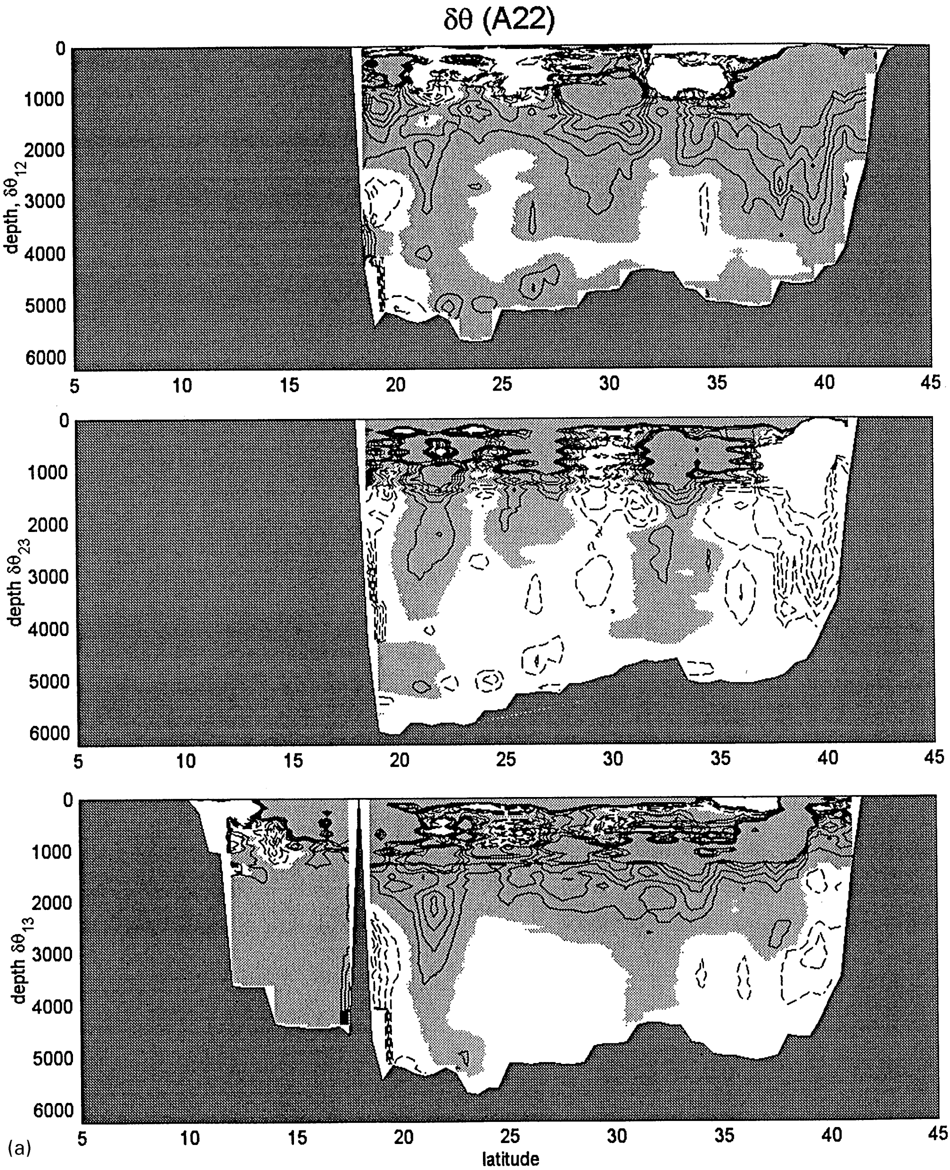

Fig. 5. Same as Fig. 4 but for A22.

deformation, we choose this as it provides a more conservative estimate of the degrees of freedom in our section means.

Averages for the latitude band between 20 and 35°N provide both an estimate of any broad scale change as well as error estimates for the mean. We will later limit our attention to only those changes that exceed one standard error of the mean (67%

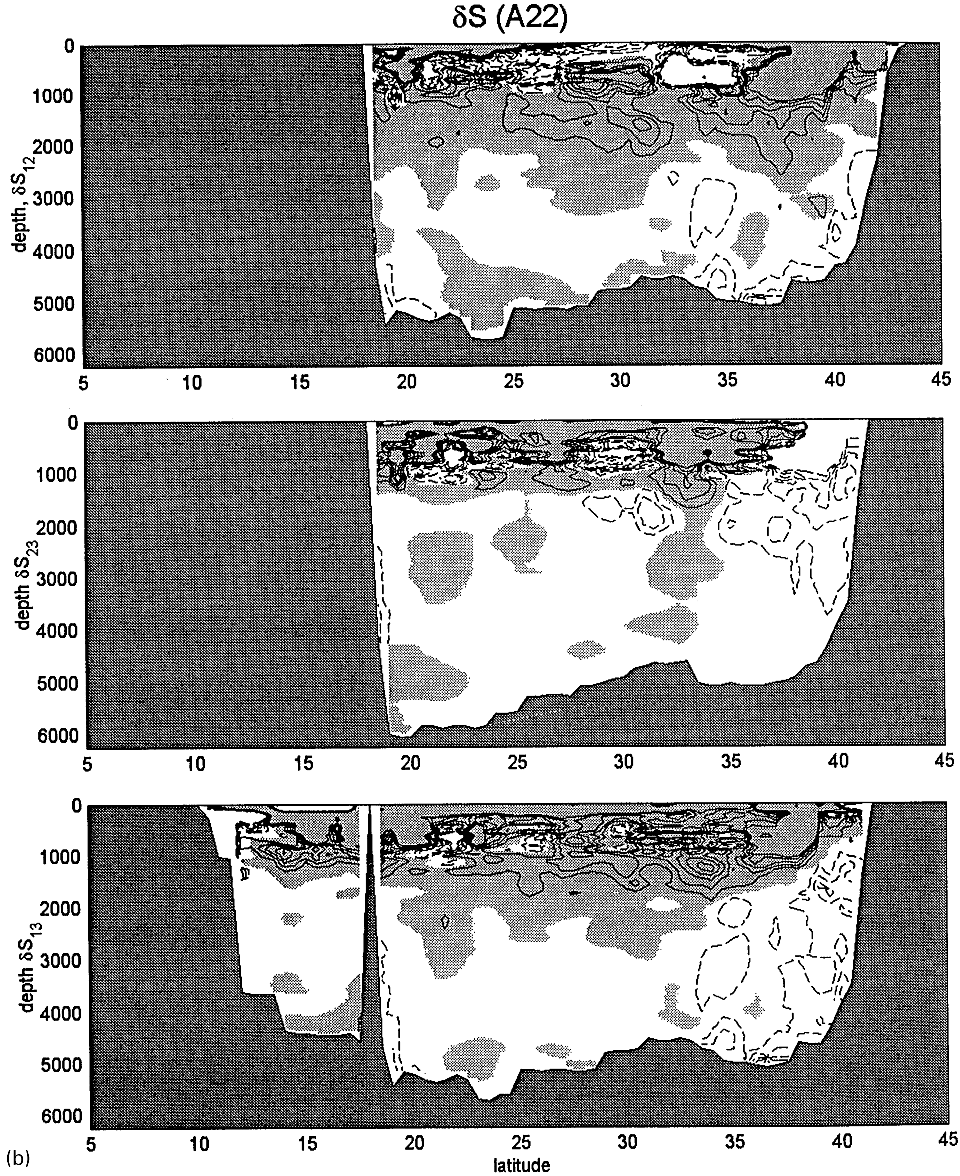

Fig. 5. Continued.

confidence limit). As one can see, this will restrict our attention to only a portion of the water column, not always the same for temperature and salinity. Many of the changes evident in the latitude/depth space discussed in the previous section are more readily apparent in the mean changes (Figs. 6 and 7). Except for the LDW, the two sections track one another quite well. One can see that changes in the upper 1000 m have been

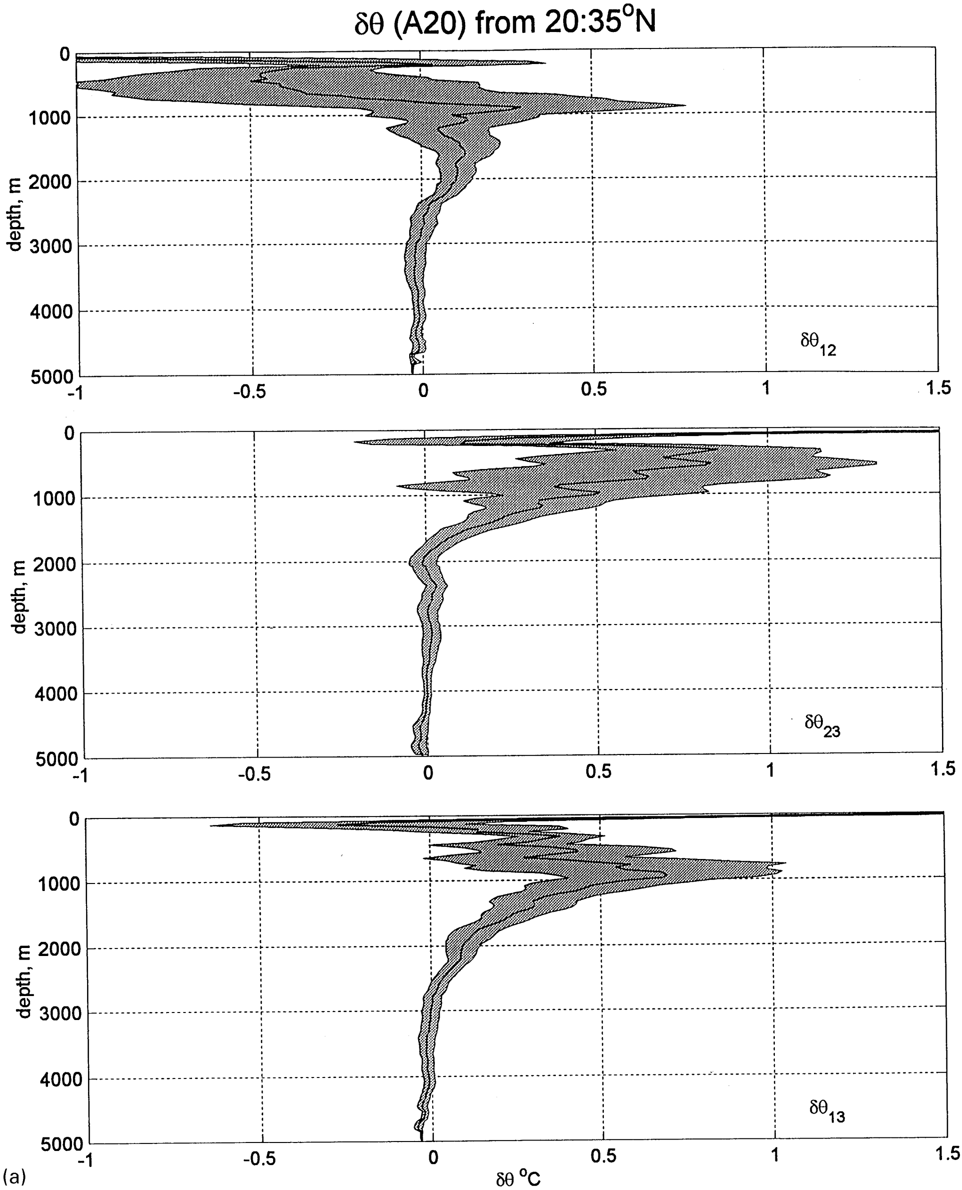

Fig. 6. Latitudinal mean differences between 20 and 35°N of potential temperature (a) and salinity (b) for A20 (52 W). Upper panel: 80s-IGY, middle: WOCE-80s, lower panel: WOCE-IGY. One standard error in the mean is shown as the gray area about the mean.

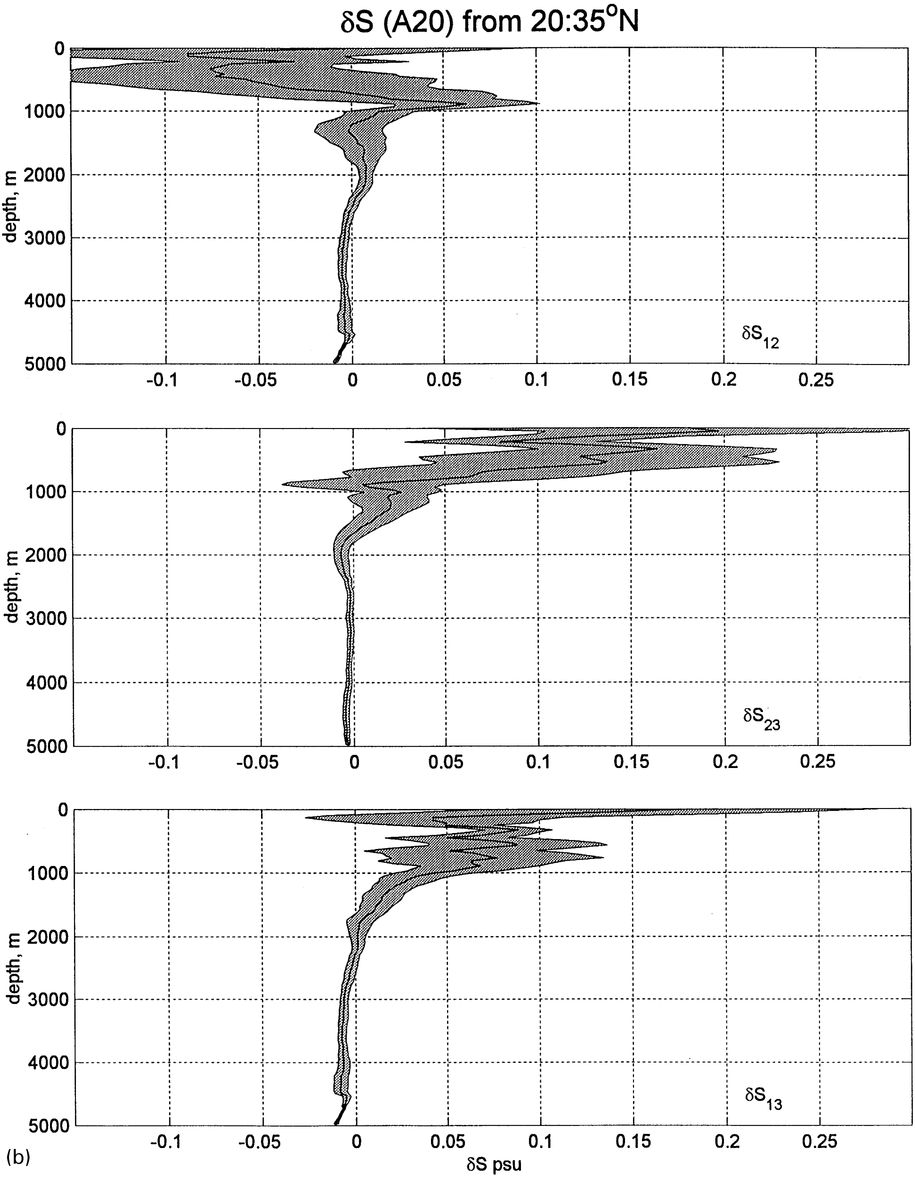

Fig. 6. Continued.

large and offsetting in the time interval IGY-80s and 80s-WOCE. This is largely due to the vertical heaving of the main pycnocline, which will be apparent later once we decompose the signal into water mass and vertical heave variability. Upper-ocean changes are also masked by large eddy variability, and this will make it difficult to diagnose the nature of the changes, since only 'significant' differences will be analyzed.

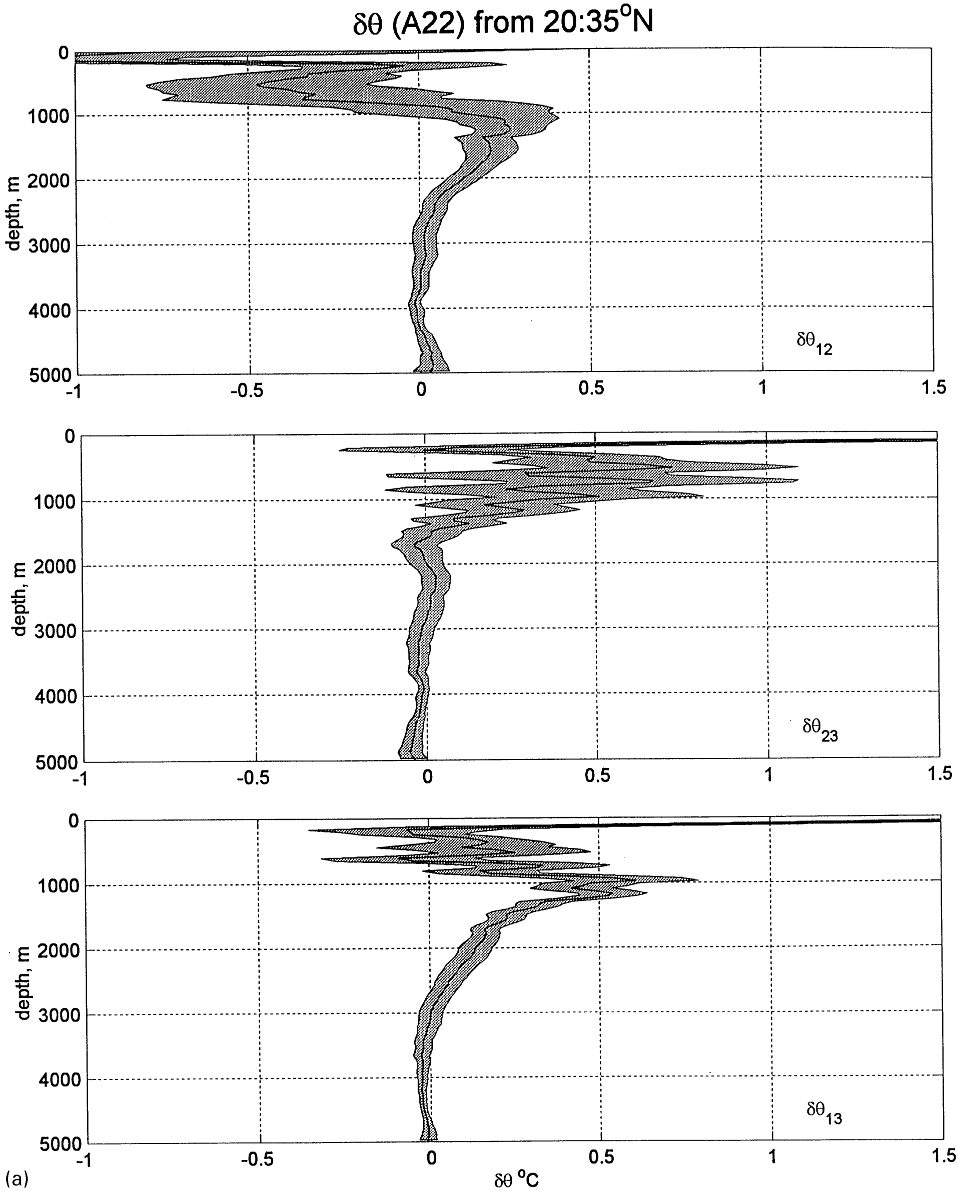

Fig. 7. As in Fig. 6, but latitudinal mean differences between 20 and 35°N of potential temperature (a) and salinity (b) for A22 (66 W).

Where changes have been of opposite sign, such as in the pycnocline and for the salinity at LSW depths (2000 m), there is no significant net change over time. Temperature changes between 1000 and 2000 m, however, have been of similar sign, and this is reflected in a large net temperature increase (above error estimates) at these depths.

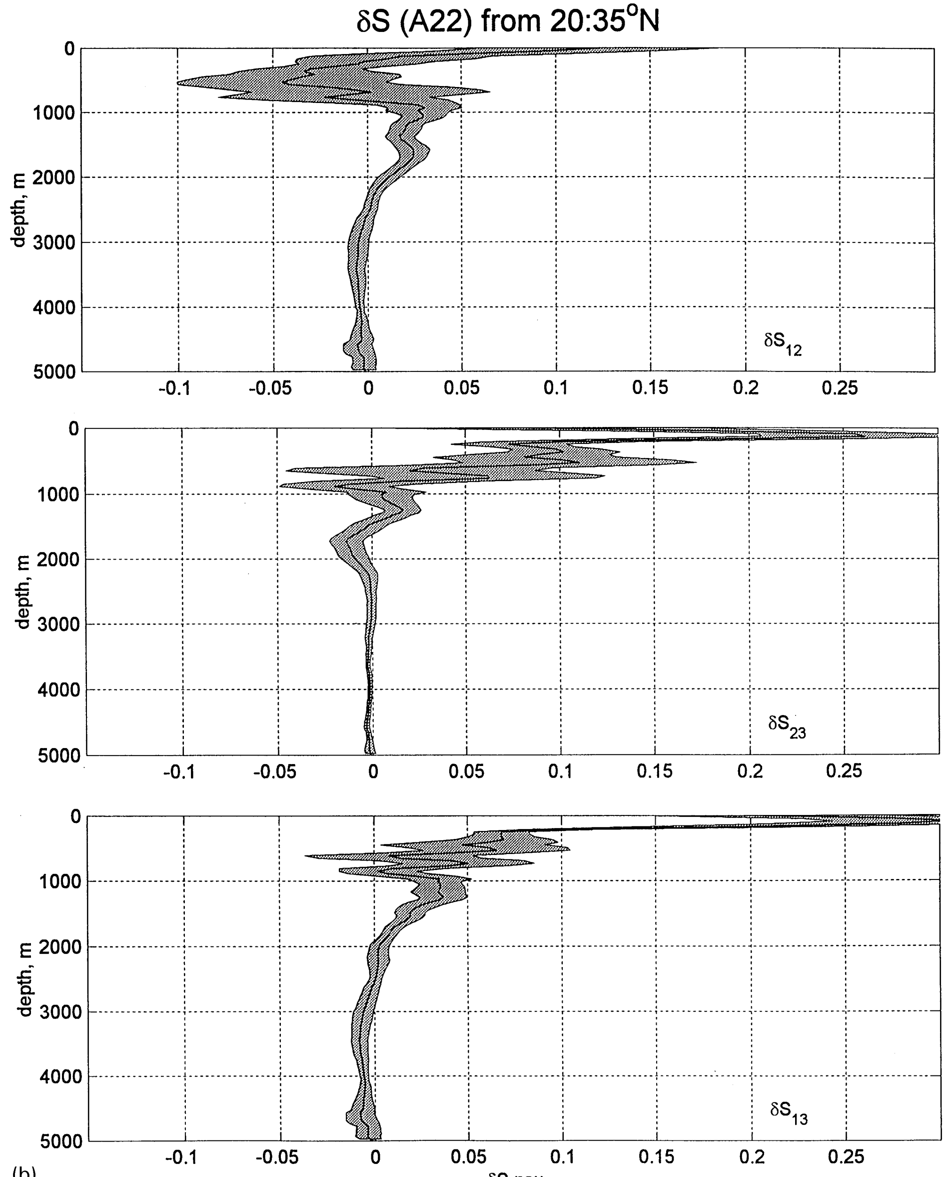

Fig. 7. Continued.

We make a departure from analysis of changes with respect to depth by showing the mean potential temperature/salinity profile for each of the occupations (Figs. 8 and 9). Since all depth information is lost in this type of display, we have indicated with symbols the properties at selected depths (200, 500, 800, 1000, 1500, 2000, 3000 and

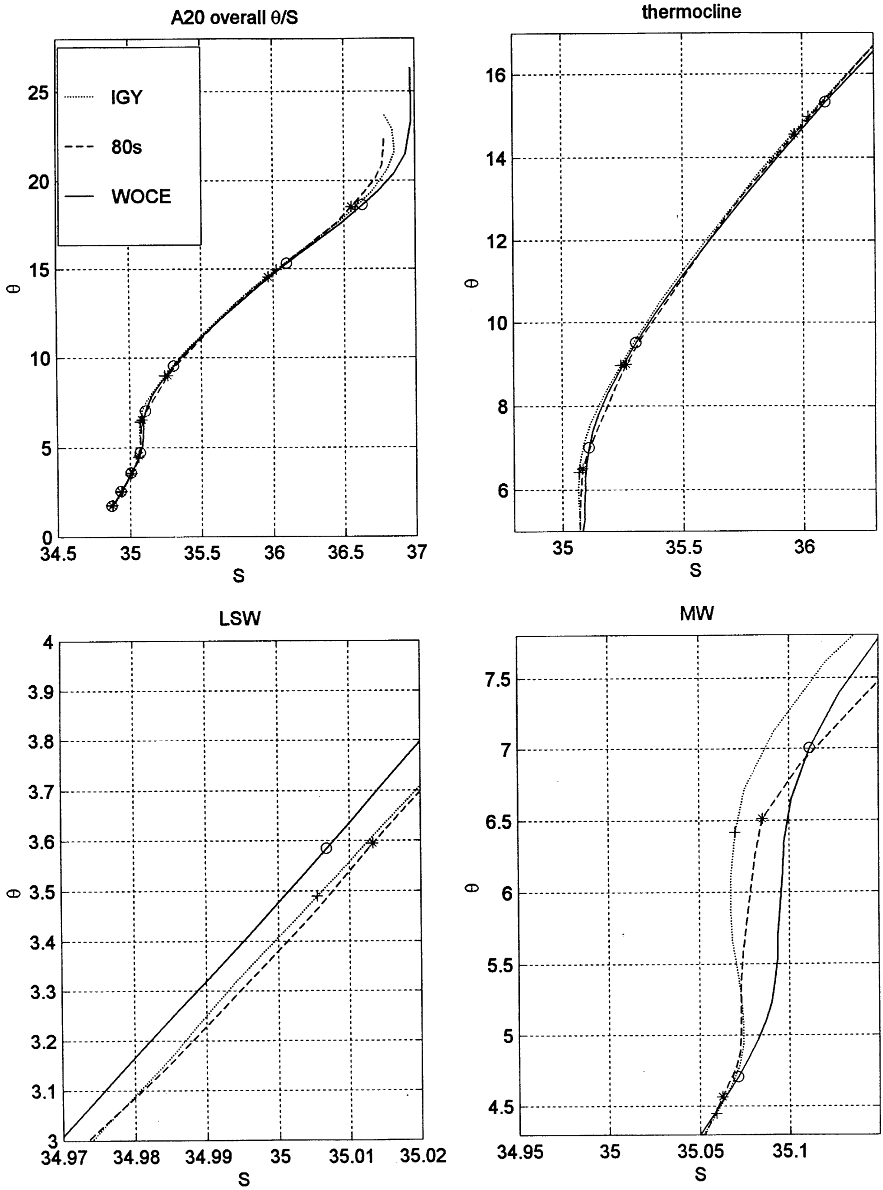

Fig. 8. Potential temperature/salinity diagrams for A20: overall (upper left), thermocline (upper right), MW (lower right) and LSW (lower left). As discussed in text, symbols denote properties at particular depth surfaces.

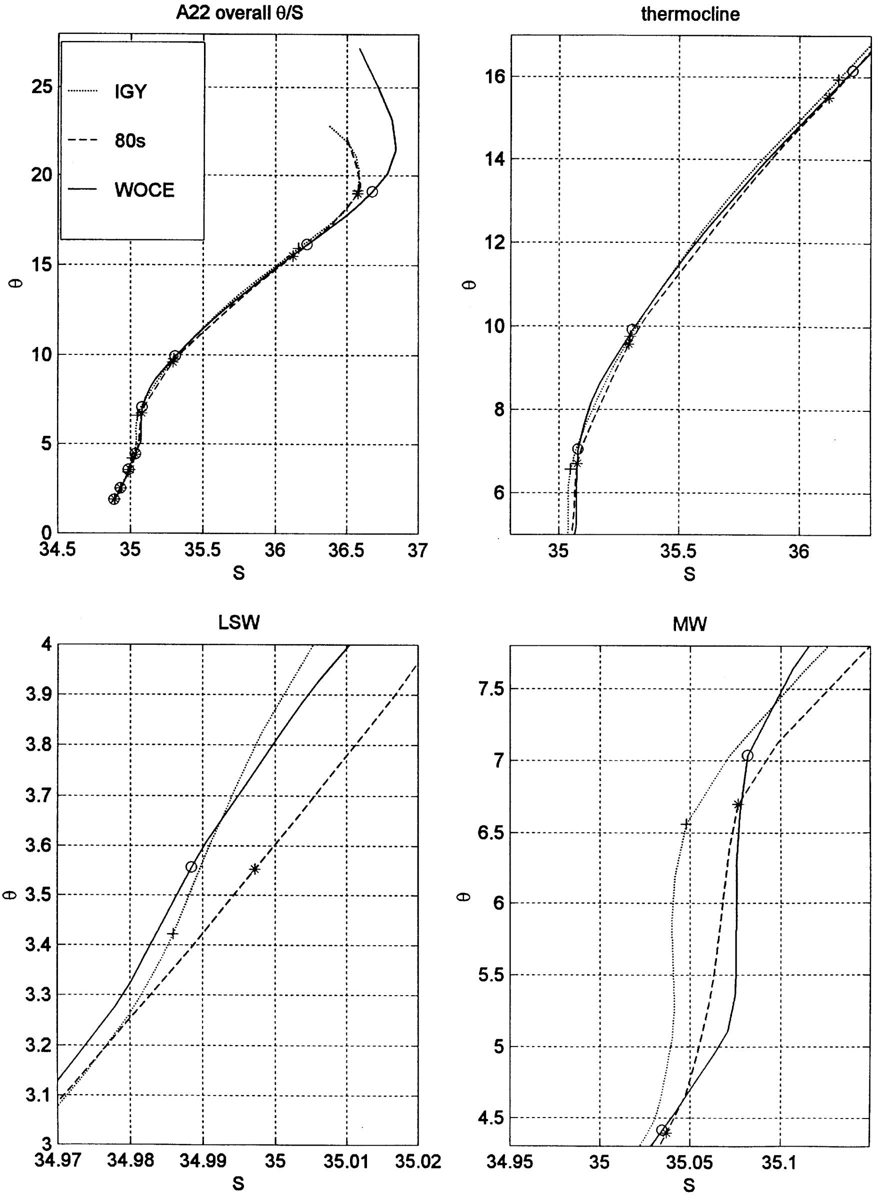

Fig. 9. Same as Fig. 8, but for A22.

4500 m). We show the overall θ/S structure in the upper left panels of both figures and selectively focus on the thermocline (upper right), MW/salinity maximum (lower right) and LSW (lower left). One change not obvious from the previous figures is the salinity increase in the upper thermocline between the first two occupations and the present.

At a depth of 200 m (first symbol on figure) this is evident as a shift of the θ/S diagram to higher salinities, while at 500 m depth, it is more clearly a change along the mean θ/S diagram. The latter type of variability characterizes much of the change throughout the thermocline between depths of 500 and 1000 m (upper right panels in Figs. 8 and 9). A change of this character indicates that the basic θ/S property change is due to a downward motion of the basic water masses due to 'heave'. This contrasts markedly with deeper changes that indicate major shifts in the θ/S structure with a progressive increase in salinity between potential temperatures of 5–6°C. In addition to this salinity increase with time, we note by the property change at 1000 m (denoted by the symbols in the upper portion of the lower right panels of the θ/S diagrams), that the potential temperature at this depth is progressively warming. From the net change between IGY and WOCE, this depth can be seen to have the maximum change in the mean $\delta\theta$ profiles (Figs. 8 and 9) discussed previously. For the LSW, changes are greater on the 66°W section (A22), as can be seen by comparison of the salinity differences in the lower left panels of Figs. 8 and 9. For both sections, the θ/S curves are coincident for the IGY and 80s near $\theta = 3.1°\text{C}$, but at the core level of the LSW (note the symbols for 2000 m depth in both), one notices a difference in character: from IGY-80s, the change indicates a θ/S shift along the mean curve for A20 but more of a combined contribution due to vertical sinking of properties as well as a salinity increase for A22. Between the 80s and the present, temperature has changed little but salinity has decreased on both sections.

3.3. *Diagnosis of changes due to heave and on neutral surfaces*

Bindoff and McDougall (1994) suggested that changes in hydrographic properites should be diagnosed in terms of changes due to vertical advection of neutral surfaces (heave) and changes on a neutral surface. This physically separates a contribution due to adjustments of the density field, which could be due to volume changes, eddies and long-period planetary waves from a passive 'dye' advected by the flow. A similar decomposition was made by Arbic and Owens (1997, personal comm.) in their analysis of some of the historical hydrographic data in the Atlantic. In terms of a representative property C, this can be written as follows:

$$\delta C = \delta C_{\mathrm{n}} + \delta C_{\mathrm{h}} + \varepsilon,$$

$$\delta C_{\mathrm{h}} \equiv -\overline{C_z} \cdot \delta z,$$

$$\delta z \equiv -\delta\gamma_{\mathrm{n}}/\overline{\gamma_{\mathrm{n}z}}$$

where the overbars refer to mean vertical gradients of the property C and neutral density $\gamma_{\mathrm{n}z}$ ($\delta z, \delta\gamma_{\mathrm{n}}$) refer to the vertical heave and observed neutral density change at depth z, respectively, and ε represents other, unmodeled dynamics such as lateral advection of existing gradients. We will use this decomposition, but normalize the first equation by the magnitude of the observed property change $|\delta C|$. In the absence of any competing process, the contributions of vertical heave and change on neutral surfaces should add up to $+1$ for a property increase with time and -1 for a property decrease. We choose to display the results (Fig. 10) only when the magnitude of the observed change is significantly greater than our estimate for the error in the mean (approx. 67% confidence level). The results for temperature and salinity differ in that the magnitude and relative error of the change are different for each variable and because the mean vertical gradients for each variable differ. For example, the contribution due to heave for salinity change at depths of the MW is small since the vertical gradient of salinity is negligible for this layer. We show the analyzed results as a function of neutral density.

The overall character of the above decomposition indicates that the two 'processes' account for nearly all of the observed changes at all levels. Within the density range of the STMW (γ_n near 26.5), the first comparison shows that an upward heave dominates the change, creating a negative temperature and salinity change, while the second comparison (WOCE-80s) shows a downward heave and corresponding temperature

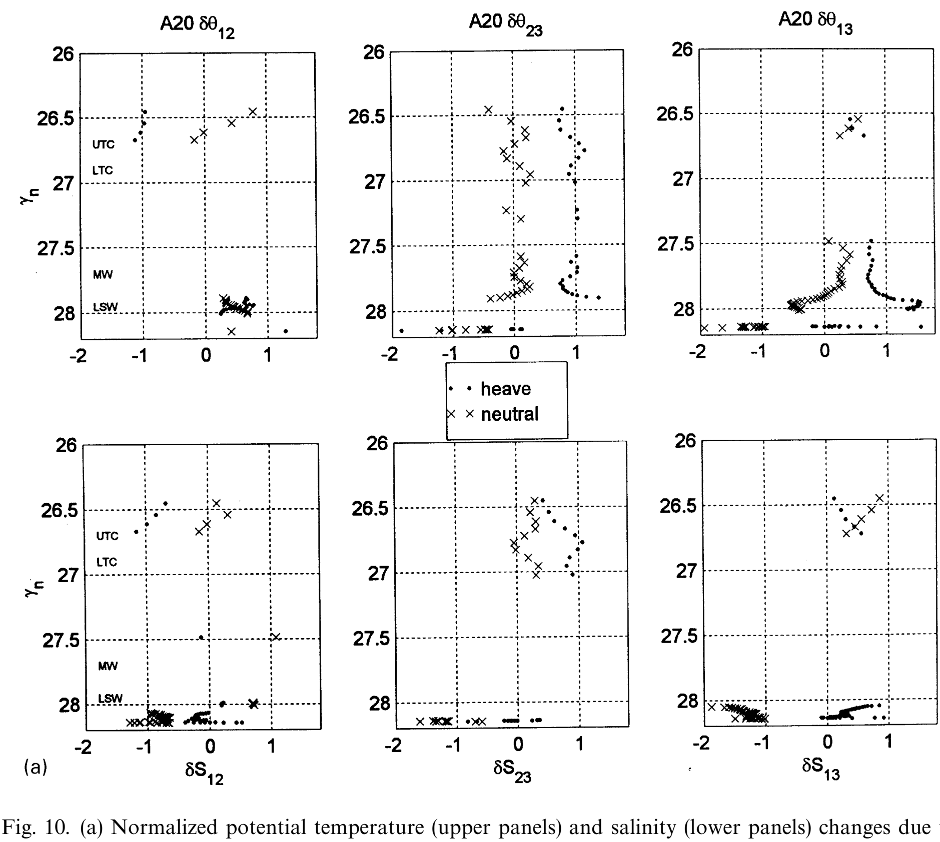

Fig. 10. (a) Normalized potential temperature (upper panels) and salinity (lower panels) changes due to heave (dots) and on neutral density surfaces (xs). In each, only significant variations are analyzed for 80s-IGY (first column), WOCE-80s (middle column), WOCE-IGY (right column) for A20 and similarly for A22 (b).

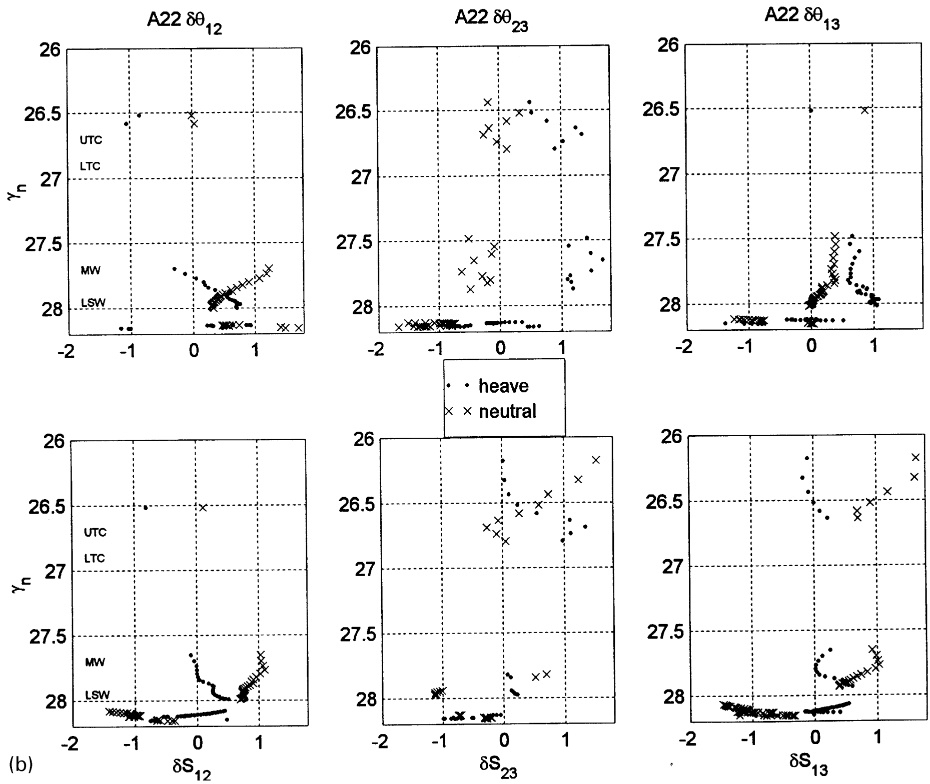

Fig. 10. Continued.

and salinity changes of opposite sign than the earlier comparison. This heave signal is due to the decadal variability of the pycnocline depth, which is most probably related to decadal changes in wind-forcing (Sturges and Hong, 1995) over the subtropical gyre. The net change suggests that both heave and neutral density changes contribute, with the latter being more dominant at shallower density levels and for the A22 section. The lower thermocline (γ_n near 26.8–27.0) shows no significant change from the IGY to the 80s, but recent changes support our earlier assertion (based on the θ/S curves above) that a negative heave (deepening of density surfaces) accounts for the observations. At the level of the MW (γ_n near 27.7), a negative heave is responsible for the temperature change on A20, but there are no significant salinity changes, that can be diagnosed. On A22, however, salinity changes are more significant with neutral surface changes, the principal agent for salinity increase, but both processes are necessary to explain the change in temperature. We noted earlier that heave would be relatively unimportant at this level for salinity because of the small vertical salinity gradient. The LSW, near $\gamma_n = 27.95$, shows the importance of both processes between the IGY and the 80s, as well as the IGY to the present. However, the significant changes from the 80s to the present are limited mainly to the A22 section and clearly show the evidence for a freshening on neutral surfaces (Fig. 10b, lower middle panel) that were clear in the θ/S curves (Fig. 9, lower left panel) for the LSW. The recent LSW change is most clearly revealed in the 66W section (A22) for the latitudinal means, although both sections show the freshening and cooling near the northern boundary. We will come back to this point in the next section. Finally, the deepest layer of LDW ($\gamma_n > 28.1$), is dominated by a freshening and cooling on neutral surfaces for the A20 section, but with the changes on A22 less significant and not clearly attributable to any single process.

4. Discussion

4.1. Net long-term changes in the subtropical gyre

Both sections show the continued warming at mid-depths in the N. Atlantic subtropical gyre, with warming most prominent at depths of 1000–1200 m, but significant warming over a wider depth interval of 800–2500 m depth (as also found on 24°N by Parrilla et al). In the face of decadal variability associated with changes in the source waters of the Labrador Sea, for example, the detection of any long-term trend is easier when individual time-series (such as at Bermuda's station '*S*') are longer or comparisons of hydrographic sections are made over greater time intervals. Spanning a time interval of about 43 years (WOCE-IGY), we see a maximum temperature increase of 0.6°C, which is nearly 1.4°C/century. Over the depth range where a significant temperature change has occurred, the net change from IGY to present is 0.25°C (A20) and 0.24°C (A22), which works out to an increasing temperature of 0.57° C per century over a depth interval of 1700 m. The net steric sea level rise can be computed from the combined contributions due to temperature and salinity. Changes in the latter will act to reduce the net sea-level increase, but the overall steric increase, accounting for changes between 800 and 2500 m depth, is 4.7 and 4.3 cm for A20 and A22, respectively, which is equivalent to about 1 mm/yr. These figures for sea level and mean temperature change are only slightly greater than those estimated from Bermuda by Joyce and Robbins (0.5°C per century and 0.7–0.9 mm/yr) but apply to a thicker water column and point to a long-term increase in the stratification between mid-depths and the underlying deep waters. We have combined the changes for both section averages (thus reducing the estimated uncertainty by sqrt(2)) and show these net changes from the IGY to WOCE in Fig. 11. The mid-depth increase in temperature and salinity is dominantly due to heaving. The depth variation of the 'heave' signal (Fig. 12) indicates a maximum negative shift of 112 m at a depth of 1800 m, giving a downward vertical velocity of the density surface at 1800 m depth of − 2.7 m/yr. The net change from IGY to WOCE tends towards zero at the surface and near the bottom. It should be noted that this heave signal is comparable to the vertical velocity expected from abyssal mixing arguments with bottom water upwelling uniformly over the ocean (Warren, 1981) but of opposite sign! One can conclude that the density field of the abyss must be far from any 'steady-state' balance between vertical upwelling and downward diffusion.

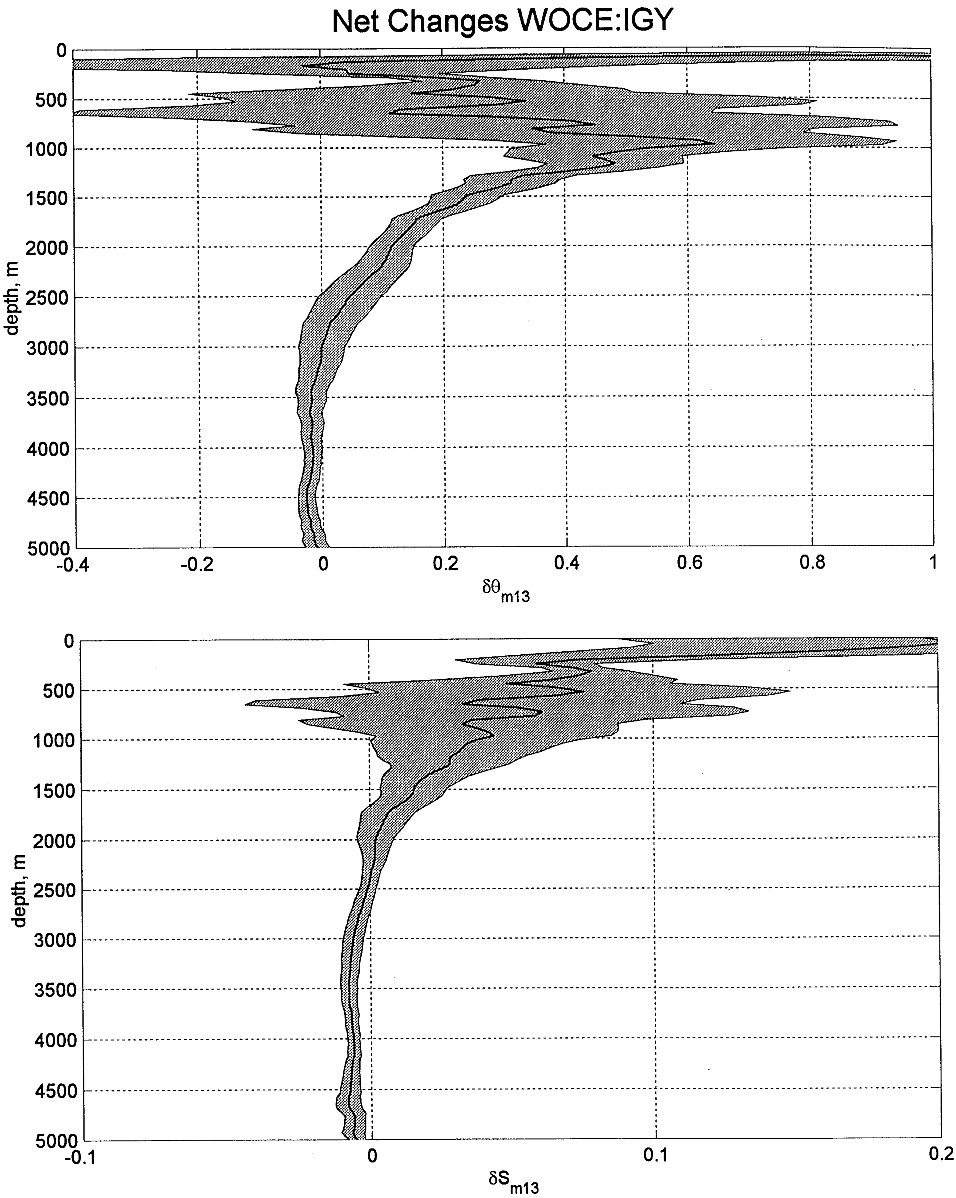

Fig. 11. Net change from IGY to WOCE of potential temperature (upper) and salinity (lower) for the combined section averages as shown in Figs. 6 and 7. One standard error is given by the gray area about the means (solid lines).

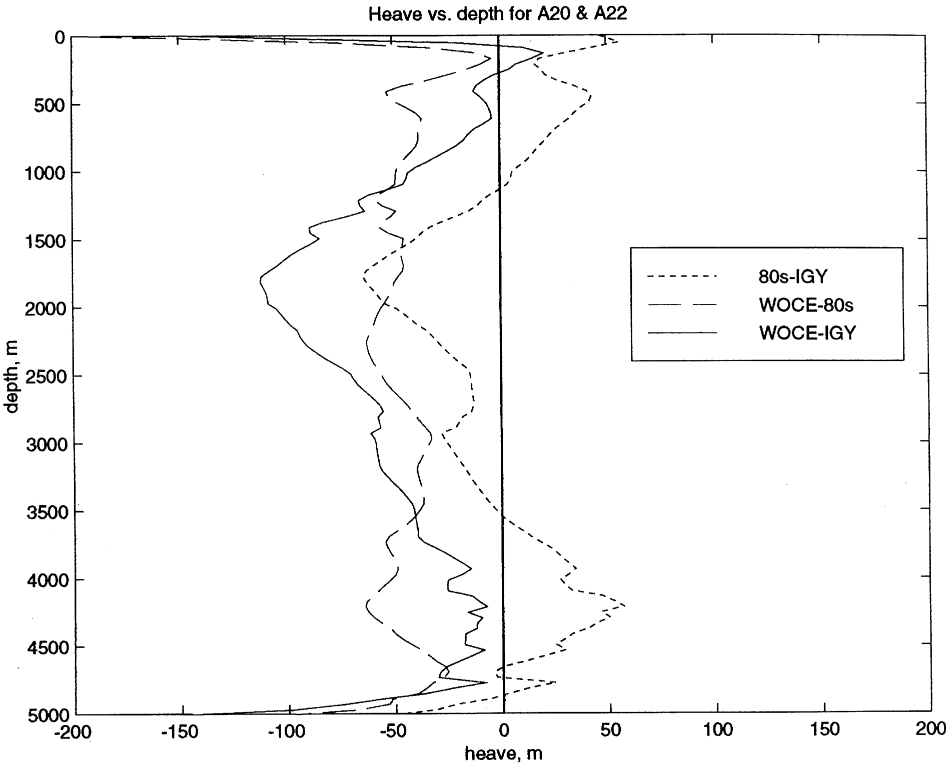

Fig. 12. The 'heave' component (calculated from neutral density) is shown for the combined section averages for each of the three comparisons. Estimates in the deep water are more subject to error because of a low vertical density gradient. Offsetting values in the upper and deep water are nearly equal giving a net change from the IGY to WOCE of small amounts. At mid-depths, the two individual comparisons add together to produce a large net negative heave with a maximum negative value of -112 m at 1800 m depth.

4.2. Changes in the Labrador Sea Water

The LSW sits within the region of maximum downward heave in the subtropical gyre. We have shown that the LSW changes are more significant on A22 than A20, and that between the 80s and WOCE this layer had undergone a significant freshening and cooling. On the latter point, it should be noted that no significant temperature change was observed on this section between the 80s and WOCE (Fig. 10b, upper middle panel), while the salinity (and thus potential temperature) decreased on neutral surfaces (lower middle panel, Fig. 10b). In this instance, heave (Fig. 12) and neutral change must offset in potential temperature, but heave contributes little to salinity change due to the low salinity gradient at this depth. Roemmich and Wunsch (1984) pointed out that the downward heave at this depth would lead to a noticeable change in the depth of the 4°C potential temperature surface. It is even more apparent in density.

We show the meridional variations in properties of the LSW on its core density (27.95 kg/m^3, Fig. 13) for both sections. As the low salinity source for LSW is in the Deep Western Boundary Current (DWBC) at the northern end of both sections, it is not surprising that the freshest LSW can be seen there. As the DWBC hugs the topography on its way south, one again encounters it on the southern ends of both sections. Differences between the two meridians are small on both the northern and southern boundaries, but the 52 W section is about 0.04 psu saltier in mid-basin due greater amounts of MW. In addition, one can see that mixing with the MW has made the LSW source waters saltier at the southern end of both sections. Because the inter-cruise variability in the LSW at the southern boundary is small on both sections, either the recent input of fresh LSW has not yet reached there or any variability present must be damped out with distance from the source. As we earlier diagnosed, heave is significant and affects mainly temperature, and the recent WOCE sections stand out as having the deepest depth of the 27.95 surface as well as the lowest temperature and salinity in the northern half of the basin. We see, however, that the MW influence is stronger in the central basin and meridional gradients are large on either side of the MW salinity maximum. Bryden et al. (1996) argued that changes in the MW at 24°N were not consistent with lateral advection as an unresolved process in their analysis, although as we see, there are significant gradients at that latitude. Eddies, acting to stir existing gradients on neutral surfaces, will produce synoptic water mass variability where mean gradients exist. As lateral gradients are larger at 52 W for the LSW layer (and the MW layer, 27.7), we believe that the detection of change is more difficult at 52 W than 66 W due to a lower signal to noise ratio. Further, if the change is mainly due to LSW, the 66 W section will show it better as it contains a higher percentage of LSW over MW.

Decadal signals within the subtropical gyre are reflected in the differences in changes between the different epochs. We have seen how the LSW warming between the IGY and 80s has come to a halt in WOCE. Curry et al. (1997) have argued that changes in convection in the source region of LSW can be seen in the subtropical gyre at Bermuda with a six year time lag. The recent cooling and deepening of LSW in the Labrador Basin began around 1990 (Pickart et al., 1997) and we expect that this signal, now appearing in the subtropical gyre, is responsible for our findings in WOCE. The Bryden et al. section in 1992 found temperature still to be increasing at 2000 m depth and for salinity to be increasing on neutral surfaces. The recent injection of cooler, fresher LSW into the subtropical gyre since 1992 would explain these observations. It also points out problems with a 'WOCE era' climatology for the N. Atlantic spanning major LSW changes.

4.3. Changes in the Lower Deep Water

At the southern end of the 52 W section, but not next to the southern boundary where boundary effects (e.g. differences due to different locations of sections relative to one another) become important, the deepest and coldest brand of LDW can be seen to be warming and getting saltier (Fig. 4a and b) with time, while further to the north, the opposite is occurring. We have shown results only for the northern region in our

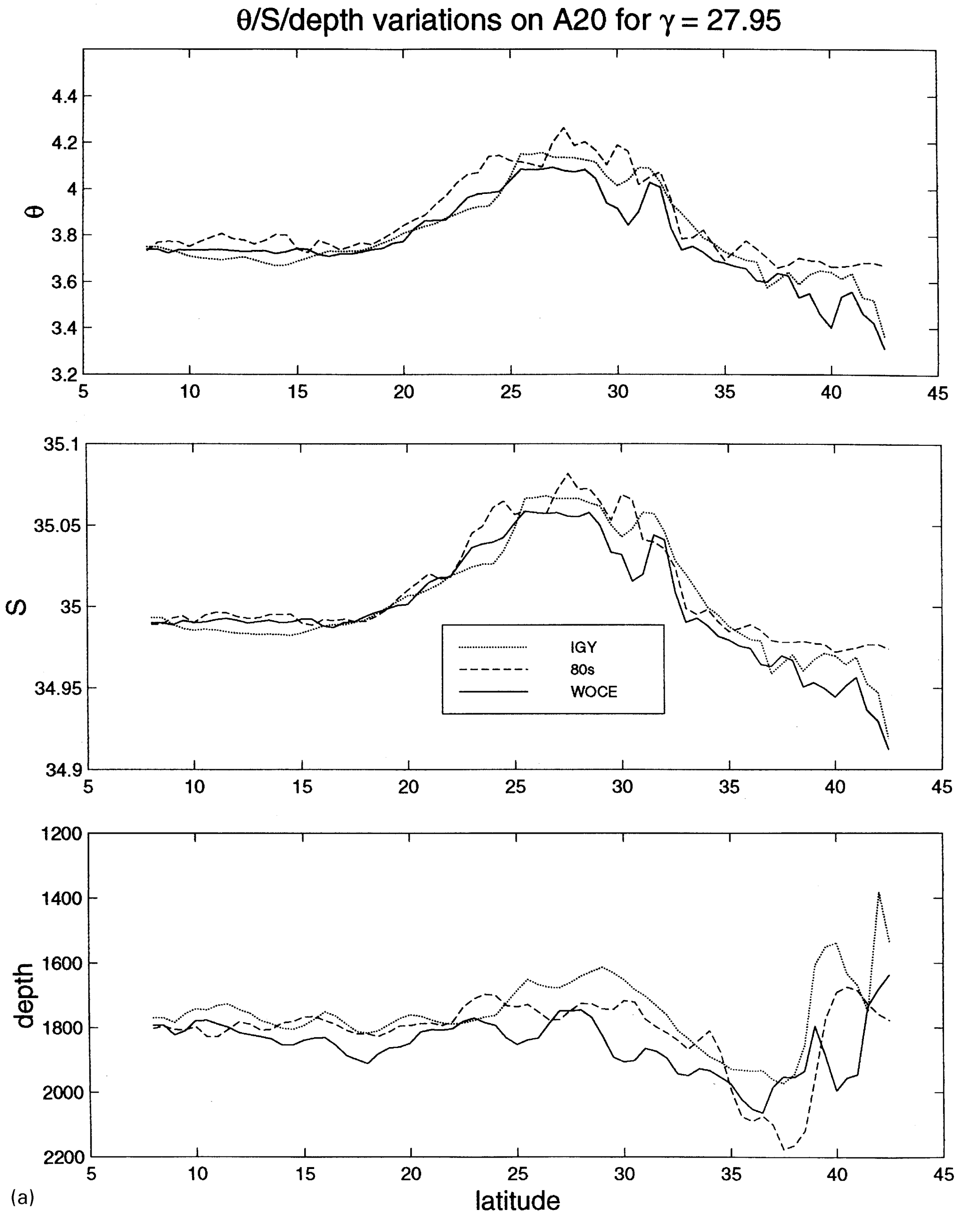

Fig. 13. Variations of potential temperature (upper), salinity (middle) and depth (lower) on the neutral density $\gamma_n = 27.95$ at the core of the LSW for A20 (a) and A22 (b).

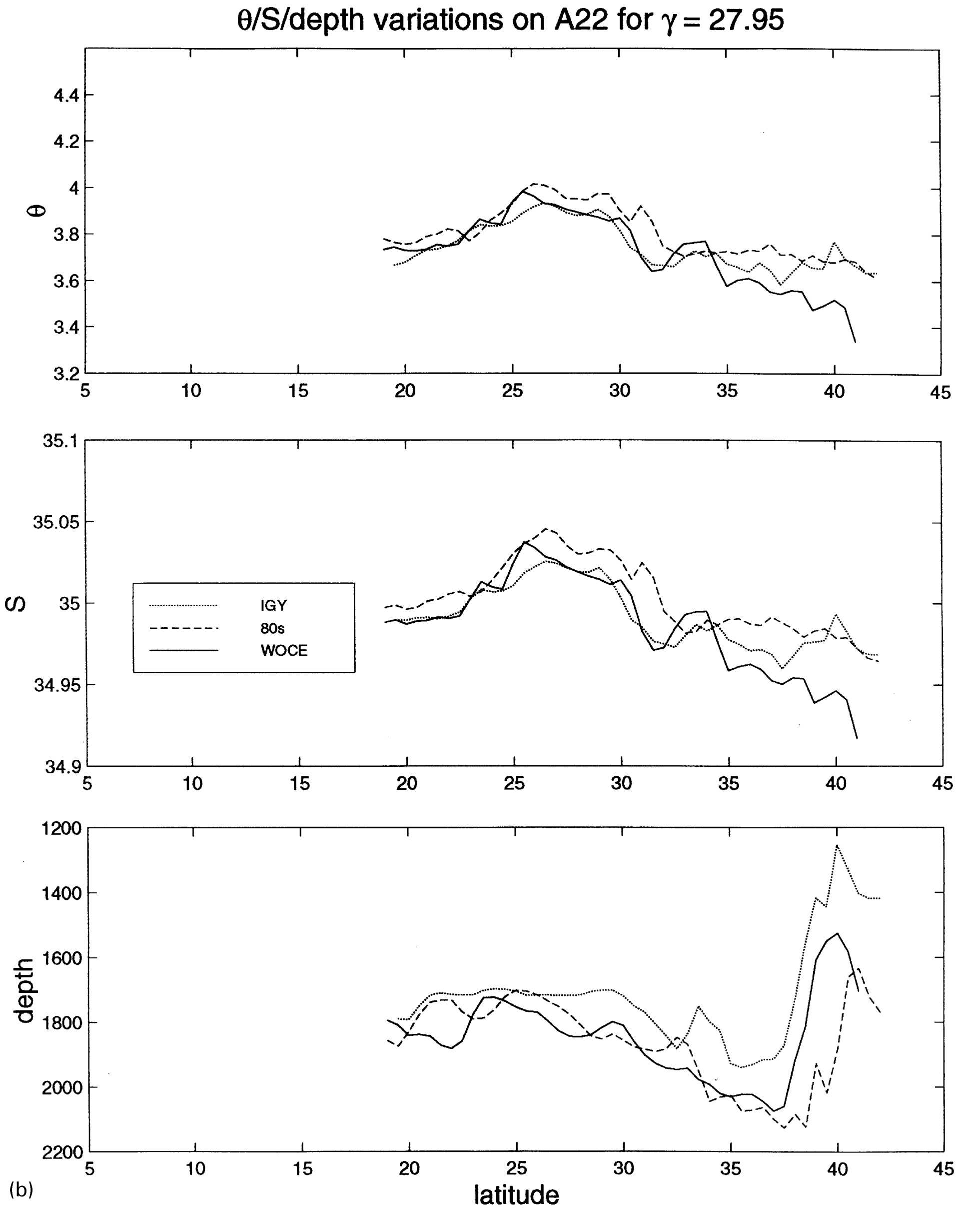

Fig. 13. Continued.

latitudinal average, but in both regions, the dominant change is a cooling and freshening on density surfaces. To the south, both salinity and temperature are increasing at a fixed depth due to the downward heaving of density surfaces (not shown). Had we combined both regions together in our latitudinal averaging, the net signal would have been reduced. This was the case on the 66 W section, which was also more problematic because of obvious 'boundary effects' (see the large positive and negative anomalies just to the north of Puerto Rico in Fig. 5a). We therefore will focus on the 20–35°N average properties for the 52 W section in our discussion of LDW change because it shows a significant freshening and cooling on neutral density surfaces over time.

A θ/S plot (Fig. 14) for the LDW along 52 W shows a progressive freshening of the LDW between the IGY, 1983 and 1997 of -0.003 psu between each of the cruises. This is a significant change only for the recent comparison and consistent with the change since the IGY, but one wonders if the IGY data can be trusted given the unknown SSW used and caveats about accuracy of IGY salts (e.g. Mantyla, 1994). Source waters for the LDW come from Nordic overflows and the Antarctic. Freshening of the water masses of the Nordic overflows have been reported by Brewer et al. (1983), comparing salinity changes between the IGY era (R/V Erica Dan in 1962) and Transient Tracers (TTO) in 1980, to be 0.02 psu. Pickart and Smethie (1997) also see a freshening of these waters of 0.01 psu from 1983 to 1995 near the boundary at 55 W.

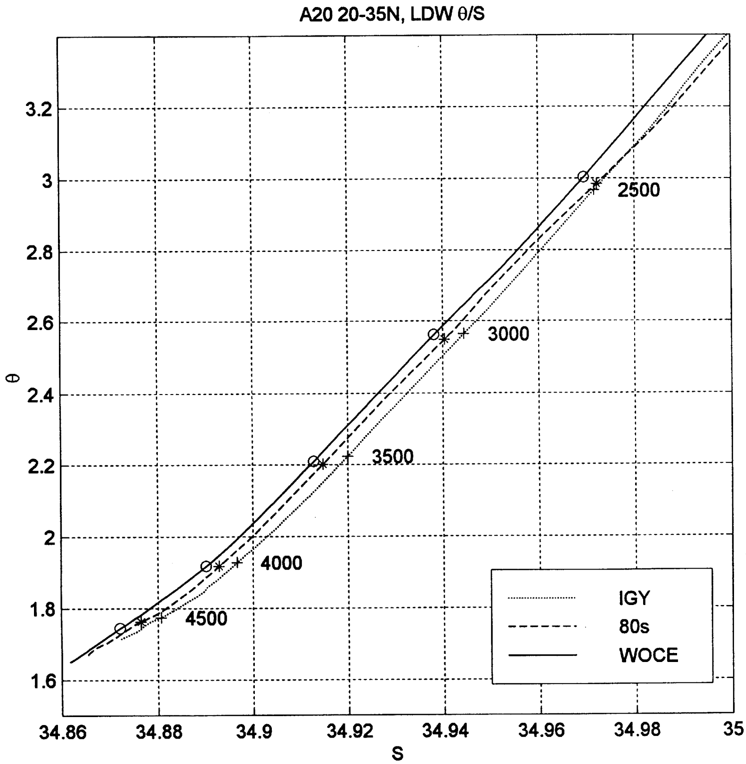

Fig. 14. Potential temperature/salinity plot of the LDW for the 52 W averages between 20 and 35°N. Selected depths are indicated in the figure for all three occupations of the section.

Antarctic Bottom Water (AABW) freshening during the early to late 1980s was observed in the Argentine and Brazil Basins by Coles et al. (1993). It is not established, however, that either of these changes in source waters is stable over time such as to produce a signal at 52 W in the N. Atlantic, nor why the signal is more prominent on 52 W than 66 W. Concerning the latter, AABW crossing the equator transposes from the western boundary to the mid-Atlantic Ridge (Speer and McCartney, 1992) and can be found at 52 W within the subtropical gyre, whereas the Nordic overflow water is concentrated along the western boundary within the gyre (Speer and McCartney, 1991). One possibility for the 52/66 W differences is that the greater variability and possible long-term freshening of the LDW observed on 52 W over 66 W may due to changes in AABW flowing into the North. Atlantic rather than to changes in the Lower North Atlantic Deep Water flowing out.

4.4. Changes in the Caribbean

The Caribbean is an interesting place to examine long-term changes, because much of the decadal variability is 'filtered out', as we will show below. Deep water flowing into the Venezuelan Basin comes through the AJ passage (Stalcup et al., 1975; Fratantoni et al., 1997), encountering a sill depth in the Anegada Passage of 1915 m and later in the Junfern Passage of 1815 m. In between these two sills is the Virgin Island Basin (VIB). In the depth range of 1800 m in the subtropical gyre outside of the VIB, we have seen the LSW to be present and changing over time, with a long-term increase in temperature but no significant change in salinity from IGY to WOCE, principally due to vertical heave. Within the Caribbean, we have calculated the mean (θ, S) changes between the IGY and WOCE eras for the latitude range of 12.5–16.5°N to be (0.041, −0.0016), respectively, with only the former being significant (Fig. 15). Although difficult to see from Fig. 5a, lower panel, the temperature change is quite uniform over the basin. As this must reflect, ultimately, the source waters, we propose a simple box model of the basin in which a volume transport, q, of source waters enters the basin with temperature T_i, and exits with the mean basin temperature of T. The 'residence time' for water in the basin is merely the ratio of the total volume, V to the inflow, or V/q, which we define as τ. If the basin starts out with temperature T_0, then the temperature balance and solution within the basin is as follows:

$$T_\mathrm{t} + \tau^{-1}T = \tau^{-1}T_\mathrm{i},$$

$$T = T_0 + \tau^{-1}\int_{-\infty}^{t} \mathrm{d}t'\; T_\mathrm{t} \exp[(t'-t)/\tau],$$

$$T_\mathrm{i} = T_0 + a\exp(t/\tau_\mathrm{i}) + b\exp(\mathrm{i}\omega t),$$

$$T = T_0 + \left[\frac{a}{1+\tau/\tau_\mathrm{i}}\right]\exp(t/\tau_1) + \left[\frac{b}{1+\mathrm{i}\omega\tau}\right]\exp(\mathrm{i}\omega\tau).$$

The first equation represents the temperature balance, the second the solution, the third a simple model for change in the source water and the fourth the solution for this

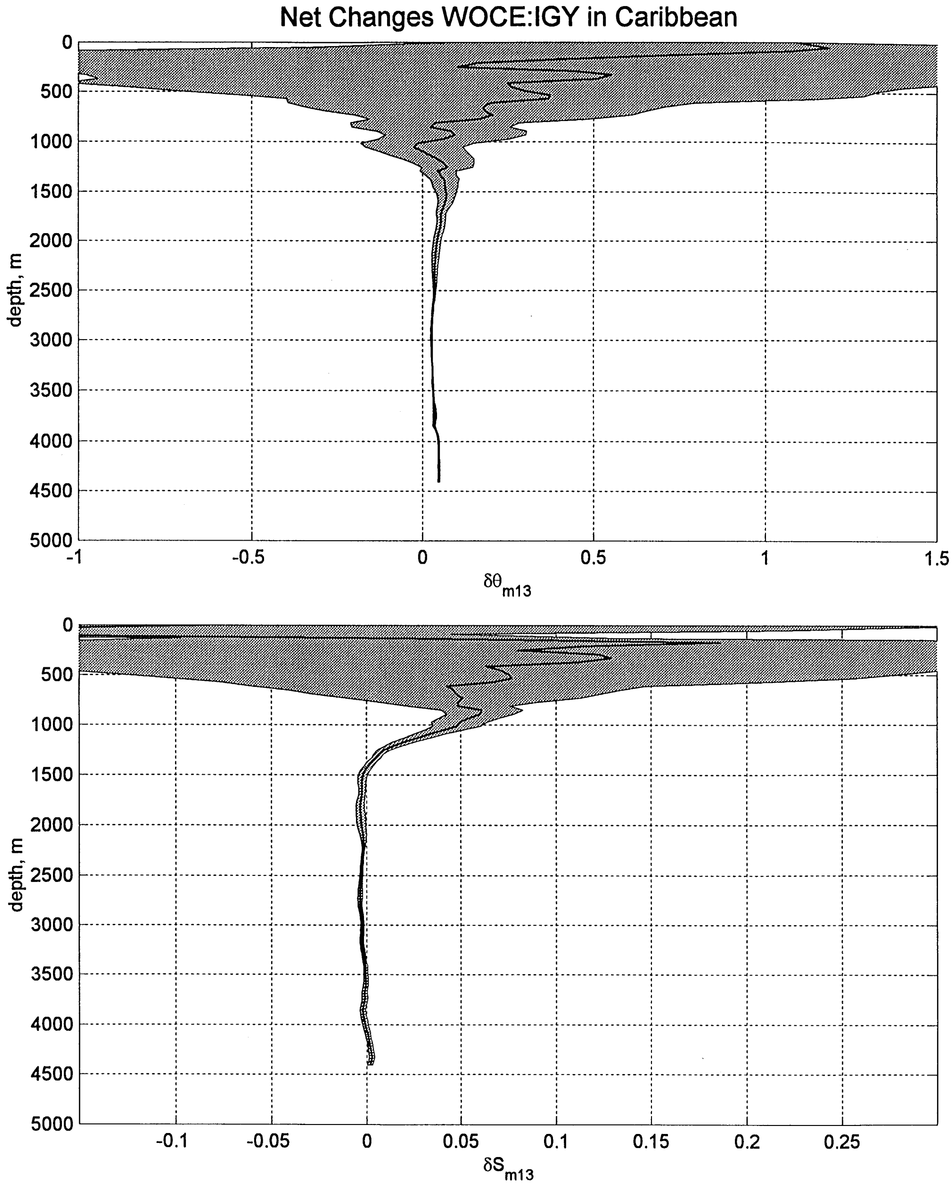

Fig. 15. Net change from IGY to WOCE of potential temperature (upper) and salinity (lower) for the latitude band 12.5 to 16.5 on 66 W (A20) in the Caribbean. One standard error is given by the gray area about the means (solid lines). At depths of the AAIW, the salinity change appears to be significantly positive but with no significant temperature change. Below the sill depth of the Caribbean, temperature (but not salinity) appears to be warming. Eddy variability masks any change in the upper waters.

Table 2
For the model of temperature change in the subtropical gyre of $a\exp(t/\tau_i)$, with a present rate of change (a/τ_i) of 0.5°C/century and a residence time of 150 ys in the Caribbean, one can calculate the expected temperature change within the Caribbean (third column) for a range of parameters. For a source that had no change prior to $t = -70$ and a steady increase at a rate of 0.5°C/century since then, we obtain the last entry in column 4

a (°C)	τ_i (yr)	δT(WOCE-IGY), (°C)
2.0	400	0.14
1.0	200	0.11
0.5	100	0.080
for $t < -70$, $T_i = 0$		
else $T_i = 0.005(t + 70)$		0.056

particular source model. The basin temperature is basically filtered by a simple single pole filter with a time constant given by τ, the residence time for the basin. With a total volume of 10^{15} m^3 and a volume transport of 0.2×10^6 m^3/s (D. Fratantoni and W. Johns, personal communication, 1997), the residence time is approximately 150 yr. Thus, the oscillatory signal for decadal time scale changes in the source waters is highly damped (by 99%) within the basin. Furthermore, any long-term trend is also reduced.

For a rate of change in the source water (at the present, or $t = 0$) of 0.5°C/century we choose a range of values of (a, τ_i) as given in Table 2. For these choices, the rate of change of temperature in the basin is reduced by a multiplicative factor ranging from 0.4 to 0.73 but still giving temperature changes (since IGY) significantly more than observed. This indicates that either the present trend in the subtropical gyre may not extend backward in time as long as that permitted by the simple exponential model or that the residence time of the Caribbean is larger by at least a factor of two.

If instead, we hypothesize that the source water began to increase in temperature 70 years ago at a rate of 0.5°C/century (consistent with Joyce and Robbins) and prior to that date was steady, then the Caribbean temperature can be calculated to be at present 0.069° C warmer than initially and 0.056°C warmer than 40 years ago (time of IGY). This model (4th row in Table 2) better describes the observations, but further tuning is not warranted given the present uncertainty in the residence time (we get perfect agreement with 215 years) and the assumption that the model transport into the basin is steady with time. Given a firm estimate of the residence time, we see that any long-term change in the LSW (with time scale $\approx \tau$) might be better measured in the Caribbean than in the Labrador Sea! Finally, we remark that geothermal heat flow from the sediments of 70 mW/m^2 (Clark et al., 1978) would warm up a water column of 2400 m thickness 0.01°C over 40 years, less than what we observe, but not entirely negligible.

5. Summary

A pair of recent WOCE hydrographic cruises occupied two meridional sections across the North Atlantic subtropical gyre at 52 W and 66 W. Combined with two earlier occupations of these meridians, this has provided an opportunity to investigate climate variability over a 40-yr time period. To avoid aliasing by lateral shifts in the Gulf Stream as well as 'high-frequency' boundary effects, we restricted our analysis to the central part of the gyre.

Temperature and salinity difference sections along the two meridians show significant changes throughout the water column. To interpret these changes better we employed a decomposition that distinguishes variation due to vertical displacement of isopycnals (heave) versus change along isopycnals (water mass variation). This, together with a *T–S* analysis, has shed light on the nature of some of the observed variability. Progressing from shallow to deep, our major findings are as follows.

The Subtropical Mode Water (18°C Water) is subject to a strong heave signal, i.e. the upward and downward displacement of isopycnals resulting in cooling and warming on depth surfaces. However, a net secular change over the entire time period appears to be due to a water mass modification (warmer/saltier), the cause of which remains an open issue. Below the mode water (roughly 1000–2000 m) we see the same general warming trend reported by Bryden et al. (1997) at 24 N. However, variation in the Mediterranean water signal at mid-depth is complex and not the same at the two meridians. Our analysis does demonstrate that any salinity change due to heave is negligible (as would be expected due to the small vertical gradients of salinity at these depths).

The most striking variation revealed by the recent WOCE occupations is in the depth range of the Labrador Sea Water (LSW). The 66 W section shows a significant cooling/freshening along isopycnals since the 80s. Such a water mass change is consistent with the recent evolution in the source history of LSW and should affect decadal changes in dissolved oxygen at these depths, as reported by Garcia et al. (1998) from 1981 to 1992. Curiously, a similar change in the LSW is not seen in the center of the gyre at 52 W, though we suspect that such variation will soon be detected there as well. Interestingly, over the entire 40 + yr time period, the LSW has become warmer and less dense, but with no significant net salinity change. This demonstrates the importance of the decadal nature of the LSW signal for salinity.

In the Lower Deep Water (LDW), which is largely a combination of Antarctic Bottom Water and Nordic overflow water, we see significant changes only at 52 W. The dominant signal is cooling and freshening on density surfaces. Note that this is in the same sense as recent changes in the LSW, but, unlike the mid-depth signal, the LDW change is confined to the east not the west. This is most likely due to a change in the Antarctic source water which flows into the North Atlantic along the Mid-Atlantic Ridge.

Finally, the deep Caribbean, which is quite homogeneous, has changed only slightly since the 1950s. The slight warming can be explained by a simple mixing model, whereby changes in the North Atlantic source water are largely damped out and shifted later in time due to the large residence time of the basin.

Acknowledgements

We wish to acknowledge the support of and NSF grant (OCE95-29607), the assistance of J. Dunworth-Baker and R. Goldsmith in helping with some of the calculations and finally, the WHOI CTD and hydro groups and the captain and crew of the R/V Knorr for their assistance in obtaining this new WOCE dataset. This is contribution number 9635 of the Woods Hole Oceanographic Institution.

References

Bindoff, N.L., McDougall, T.J., 1994. Diagnosing climate change and ocean ventilation using hydrographic data. Journal of Physics and Oceanography 24, 1137–1152.

Brewer, P.G., Broecker, W.S., Jenkins, W.J., Rhines, P.B., Rooth, C.G., Swift, J.H., Takahashi, T., Williams, R.T., 1983. A climatic freshening of the deep Atlantic north of 50°N over the past 20 years. Science 222, 1237–1239.

Bryden, H.L., Griffiths, M.J., Lavin, A.M., Millard, R.C., Parrilla, G., Smethie, W.M., 1996. Decadal changes in water masses characteristics at 24° N in the subtropical Atlantic Ocean. Journal of Climate 9, 3162–3186.

Clark, T.F., Korgen, B.J., Best, D.M., 1978. Heat flow in the eastern Caribbean. Journal of Geophysical Research 83, 5883–5891.

Culkin, F., Ridout, P.S., 1998. Stability of IAPSO standard seawater, Journal of Atmosphere and Oceanic Techonology 15, 1072–1075.

Curry, R.G., McCartney, M.S., Joyce, T.M., 1998. Oceanic transport of subpolar climate signals into mid-depth subtropical waters. Nature 391, 575–577.

Fratantoni, D.M., Zantopp, R.J., Johns, W.R., Miller, J.L., 1997. Updated bathymetry of the Anegada-Junfern Passage complex and implications for Atlantic inflow to the abyssal Caribbean Sea. Journal of Marine Research 55, 847–860.

Fuglister, F.C., 1960. Atlantic Ocean Atlas of temperature and salinity profiles and data from the International Geophysical Year of 1957–1958. Woods Hole Oceanographic Institution Atlas Series I, 209pp.

Garcia, H., Cruzado, A., Gordon, L., Escanez, J., 1998. Decadal-scale chemical variability in the subtropical Norht Atlantic deduced from nutrient and oxygen data. Journal of Geophysical Research 103, 2817–2830.

Jackett, D., McDougall, T.J., 1996. A neutral density variable for the world's ocean. Journal of Physics and Oceanography 96, 237–263.

Joyce, T.M., Robbins, P., 1996. The long-term hydrographic record at Bermuda. Journal of Climate 9, 3121–3131.

Knapp, G. P., Stalcup, M.C., 1987. Progress in measurement of salinity and oxygen at the Woods Hole Oceanographic Institution. Technical Report, WHOI-87-4, Woods Hole Oceanographic Institution, 27pp.

Lazier, J.R.N., 1995. The salinity decrease in the Labrador Sea over the past thirty years. In: Martinson, D.G., Bryan, K., Ghil, M., Hall, M.M., Karl, T.M., Sarachik, E.S., Sorooshian, S., Talley, L.D. (Eds.), Natural Climate Variability on Decade-to-Century Time scales. National Academy Press, Washington, DC, pp. 295–302.

Levitus, S., 1989a. Interpentadal variability of temperature and salinity at intermediate depths of the North Atlantic Ocean, 1970–74 versus 1955–1959. Journal of Geophyical Research 94, 6091–6131.

Levitus, S., 1989b. Interpentadal variability of temperature and salinity in the deep North Atlantic Ocean, 1970–74 versus 1955–1959. Journal of Geophysical Research 94, 6091–6131.

Mantlya, A. W., 1980. Electrical conductivity comparisons of standard seawater batches P29–P84. Deep-Sea Research 27, 837–846.

Mantlya, A.W., 1987. Standard Seawater comparisons updated. Journal of Physics Oceanography 17, 543–548.
Mantyla, A.W., 1994. The treatment of inconsistencies in Atlantic deep water salinity data. Deep-Sea Research 41, 13387–13405.
McCartney, M.S., 1992. Recirculating components to the deep boundary current of the northern North Atlantic. Progress in Oceanography 29, 283–383.
Millard, R., Bond, G., Toole, J., 1993. Implementation of a titanium strain guage pressure sensor transducer for CTD applications. Deep-Sea Research 40, 1009–1021.
Parrilla, G., Lavin, A., Bryden, H., Garcia, M., Millard, R., 1994. Rising temperatures in the subtropical North Atlantic Ocean over the past 35 years. Nature 369, 48–51.
Pickart, R.S., Smethie, Jr. W.M., 1997. Temporal evolution of the deep western boundary current where it enters the sub-tropical domain. Deep-Sea Research, in press.
Pickart, R.S., Spall, M.A., Lazier, J.R.N., 1997. Mid-depth ventilation in the western boundary current system of the sub-polar gyre. Deep-Sea Research 44, 1025–1054.
Roemmich, D., Wunsch, C., 1984. Apparent changes in the climatic state of the deep North Atlantic Ocean. Nature 307, 447–450.
Saunders, P.M., 1986. The accuracy of measurement of salinity, oxygen and temperature in the deep oceans. Journal of Physics Oceanography 16, 189–195.
Speer, K.G., McCartney, M.S., 1991. Tracing the North Atlantic deep water across the equator. Journal of Geophysical Research 96, 20 443–20 448.
Speer, K.G., McCartney, M.S., 1992. Bottom water circulation in the western North Atlantic. Journal of Physics and Oceanography 22, 83–92.
Stalcup, M.C., Metcalf, W.G., Johnson, R.G., 1975. Deep Caribbean inflow through the Anegada-Junfern Passage. Journal of Marine Research Supplement 33, 15–35.
Warren, B.A., 1981. Deep circulation of the world ocean. Evolution of Physical Oceanography. MIT Press, Cambridge, 623 pp.
Worthington, L.V., 1959. The 18°C water in the Sargasso Sea. Deep-Sea Research 5, 297–305.